

UNIVERSITY OF TECHNOLOGY, SYDNEY

Nondestructive Evaluation of Ferromagnetic Critical Water Pipes Using Pulsed Eddy Current Testing

by

Nalika Ulapane

A thesis submitted in partial fulfillment for the
degree of Doctor of Philosophy

in the
Faculty of Engineering and IT
Intelligent Mechatronic Systems Group

February 2016

Production note:

Access to the full text of this thesis is restricted due to the inclusion of 3rd Party Copyright material. This version includes only the introduction, literature review and reference list.

Declaration of Authorship

I, Nalika Ulapane , declare that this thesis titled, ‘Nondestructive Evaluation of Ferromagnetic Critical Water Pipes Using Pulsed Eddy Current Testing’ and the work presented in it are my own. I confirm that:

- This work was done wholly or mainly while in candidature for a research degree at this University.
- Where any part of this thesis has previously been submitted for a degree or any other qualification at this University or any other institution, this has been clearly stated.
- Where I have consulted the published work of others, this is always clearly attributed.
- Where I have quoted from the work of others, the source is always given. With the exception of such quotations, this thesis is entirely my own work.
- I have acknowledged all main sources of help.
- Where the thesis is based on work done by myself jointly with others, I have made clear exactly what was done by others and what I have contributed myself.

Nalika Ulapane

28 January, 2016

UNIVERSITY OF TECHNOLOGY, SYDNEY

Abstract

Faculty of Engineering and IT
Intelligent Mechatronic Systems Group

Doctor of Philosophy

by Nalika Ulapane

Modern day maintenance of infrastructure demands significant attention to structural health monitoring. Assessment of surface condition alone is insufficient for health and strength assessment, creating the necessity to evaluate the integrity of subsurface regions through Nondestructive Evaluation (NDE). This thesis focuses on approaches to solving the problem of condition assessment of critical pipes, *i.e.*, large diameter high-pressure pipes owned and managed by water utilities to distribute consumable fresh water to customers, by developing techniques for representing the geometry of electrically conductive ferromagnetic materials via Pulsed Eddy Current (PEC) sensors.

The main contribution of this thesis is a novel detector coil voltage decay rate based PEC signal feature, the fundamental behavior of the feature is analytically described and experimentally validated. The feature has a convenient advantage in practical application since it is directly extractable from raw PEC signals and demonstrates significant invariance to sensor shape, size, and lift-off. The feature behavior is exploited in two estimation approaches, in situ measurements on pipes are performed and pipe wall thickness is inferred with uncertainty.

Firstly, an analytical approach to learning a function mapping the decay rate feature to test piece thickness with the aid of signals captured on calibration blocks is presented. The requirement of fabricating calibration blocks to have material properties matching those of pipes is extremely challenging. Thus, combining ultrasound measurements together with PEC is proposed to address material variations.

Secondly, a numerical NDE semi-parametric estimation approach is presented, PEC sensor signals are simulated taking into account measured electrical and magnetic properties of materials being tested. The thickness-feature function is learned probabilistically using Gaussian Process. Unlike in the analytical approach, the function is learned non-parametrically, therefore, variations and marginal nonlinearities are captured. The advantages over the analytical approach are demonstrated in terms of improved accuracy of inferred material thickness.

Finally, the resolution of commercial PEC sensors employed on pipes is identified as a limiting factor for structural integrity assessment. A numerical study on optimizing PEC sensor architecture to achieve higher resolution while maintaining sufficient penetration capability is carried out and a framework which can be used to perform 3D profiling by means of joint inference of thickness and lift-off is proposed.

Keywords: Analytical Modeling, Critical Pipes, Ferromagnetic, Finite Element Analysis, Gaussian Process, Inverse Eddy Current Problem, Machine Learning, NDE, NDT, Pulsed Eddy Current Signal

Acknowledgements

I would like to express my gratitude to a number of people who have helped me during my Ph.D. study. Firstly, I thank my principal supervisor Associate Professor Jaime Valls Miro for his supervision and support throughout the research. I would also like to thank my co-supervisors Associate Professor Sarath Kodagoda and Dr. Alen Alempijevic for closely following, assisting and supervising me in all aspects of the research while allocating time to review my work.

Secondly, I would like to thank Professors Gamini Dissanayake and Tomonari Furukawa for their valuable insight and advice. Their experience, broad scope of knowledge and effective feedback were immensely helpful in identifying best research methodologies.

Next, I would like to extend my gratitude to the whole Critical Pipes Project research team of University of Technology Sydney (UTS), which included Dr. Teresa Vidal Calleja, Dr. Brad Skinner, Dr. Aengus Martin, Dr. Lei Shi, Dr. Qiang Zhang, Mr. Freek De Bruijn, Mr. Buddhi Wijerathna, Mr. Raphael Falque, Mr. Daobilige Su and Ms. Liye Sun, for assisting me in various aspects. If not for their tireless efforts and support, this research would not have become a possibility.

I would also like to extend my gratitude towards Rock Solid Group[®], the main technological provider for this research. Their appreciable collaboration, provision of sensors, data, and details of the sensor for modeling were a major key to research outcomes.

Special thanks should go to Prof. Besim Ben-Nissan and Dr. Gregory Heness for sharing knowledge on metallurgy in relation critical pipe materials, and Dr. Germanas Peleckis and Mr. Russell Nicholson for their assistance in providing access to laboratory measurement facilities.

Numerous workshops, laboratory facilities, work & storage spaces within and outside UTS; and tools, devices & equipment provided by different commercial and non-commercial providers were used for various purposes including, but not limited to activities such as cutting, machining, grinding, grit blasting, measuring etc. I am not able to mention by name, all the parties, and individuals who were involved in facilitating all such activities, but there is no reduction in the immensity of my gratitude towards everybody involved.

Last but not the least, my utmost gratitude goes to my parents, Mahesh & Ramya Ulapane and family for their love and care right throughout; all my previous educational institutions and their members for educating me to come thus far in academia; the staff of UTS

Graduate Research School for orientating me as a research student and smoothly managing my candidature & scholarships; the UTS Library for providing unrestricted access to literature; the staff of UTS Faculty of Engineering and Information Technology and many other departments for assisting me in various respects; and my colleagues & friends for always being with me to keep the spirits high and the energy flowing.

This thesis is an outcome from the Critical Pipes Project funded by Sydney Water Corporation, Water Research Foundation of the USA, Melbourne Water, Water Corporation (WA), UK Water Industry Research Ltd, South Australia Water Corporation, South East Water, Hunter Water Corporation, City West Water, Monash University, University of Technology Sydney and the University of Newcastle. The research partners are Monash University (lead), University of Technology Sydney and University of Newcastle.

Contents

Declaration of Authorship	i
Abstract	iii
Acknowledgements	v
List of Figures	xi
List of Tables	xvii
Abbreviations	xix
Nomenclature	xxi
Glossary of Terms	xxiii
1 Introduction	1
1.1 Background	3
1.2 Motivation	5
1.3 Scope	7
1.4 Contributions	10
1.5 Publications	11
1.5.1 Directly Related Publications	11
1.5.2 Indirectly Related Publications	12
1.6 Thesis Layout	12
2 Review of Related Work	15
2.1 EC Inspection Techniques	16
2.1.1 Principle of EC Inspection	17
2.1.2 Conventional (Single Frequency) EC Inspection	17
2.1.3 Multi-Frequency EC Inspection	19
2.1.4 PEC Inspection	20
2.2 Commonly Used PEC Sensor Architectures	21
2.2.1 Detector Coil Based PEC Sensor Architecture	21

2.2.2	Non-Detector Coil Based PEC Sensor Architecture	23
2.3	PEC Based Ferromagnetic Material Thickness Quantification	24
2.3.1	Application Specific Noise Suppression Techniques	25
2.3.2	Thickness Discriminative Feature Extraction Techniques	28
2.4	Effect of PEC Sensor Geometry on Measurement Capabilities	33
2.5	Conclusions	35
3	Detector Coil Voltage Decay Rate as a Thickness Discriminative PEC Signal Feature	37
3.1	Analytical Derivation of the Functional Behavior between Thickness and the Decay Rate Feature	38
3.2	Experimental Validation of the Behavior of the Decay Rate Feature	43
3.2.1	PEC Sensing Unit Used in this Thesis	43
3.2.2	Obtaining PEC Signals from Calibration Blocks made of Critical Pipe Materials	44
3.2.3	Experimental Validation of $\beta(t)$ Monotonicity	46
3.2.4	Extracting β_{max} from Experimental PEC Signals	48
3.2.5	Experimental Validation of the Existence of the Linear Thickness-Feature Function	52
3.2.6	Sensitivity Analysis of β_{max}	54
3.2.6.1	Low Dependence on Sensor Lift-off	55
3.2.6.2	Low Dependence on Sensor Size	58
3.3	FEA Validation of Invariance of β_{max} for Cylindrical Structures	62
3.4	Analytical NDE Framework Based On Experimentally captured Calibration Signals	65
3.4.1	Analytical Model Estimation	65
3.4.2	Using the Analytical Model for Critical Pipe NDE	66
3.4.3	Validation	67
3.4.4	Results	69
3.4.5	Limitations of the Analytical NDE Approach	70
3.5	Scaling Based Alternative Thickness Quantification Method for Critical Pipe NDE	73
3.6	Local Nonlinearities Present in the Thickness-Feature Function	74
3.7	Sensor Noise Characterization	79
3.8	Conclusions	80
4	Approach for Numerical and Probabilistic Sensor Modeling	83
4.1	Measuring Electrical and Magnetic Properties of Pipe Materials	84
4.2	Numerically Modeling the PEC Sensor	90
4.2.1	Governing Equations of the Numerical Model	91
4.2.2	Developing the Numerical Model	95
4.2.3	Results Produced by the Numerical Model	99
4.3	Non-Parametric Learning of the Thickness-Feature Function Using GP . . .	104
4.4	Probabilistic Inference of Pipe Wall Thickness	110
4.5	Comparison of GP Interpreted Results with the Analytical Approach	115

4.6	Conclusions	117
5	Towards 3D Profiling in Critical Pipe NDE	121
5.1	FEA Model Used for the Study	123
5.1.1	Developing the Model	123
5.1.2	Theoretical Verification of the Model	125
5.2	Problem Formulation for Increasing Sensor Resolution	126
5.2.1	The Base Model	126
5.2.2	Procedure for Increasing Resolution	130
5.3	Low Dependence of β_{max} on Sensor Shape	131
5.4	Finding the Domain of Influence of the Base Model	132
5.4.1	Verifying Penetration Capability	132
5.4.2	Finding Lateral (Horizontal) Domain of Influence	134
5.5	Increasing Sensor Resolution (Reducing the Domain of Influence)	135
5.6	Towards 3D Profiling	138
5.6.1	Effects of Corrosion and Graphitization Process on PEC NDE	139
5.6.2	Effect of σ_t and σ_b on the PEC signal	141
5.6.3	The 3D Profiling Framework	142
5.6.4	Results	143
5.7	Conclusions	144
6	Conclusions	147
6.1	Summary of Contributions	148
6.1.1	A Novel PEC Signal Feature for Thickness Quantification	148
6.1.2	An Analytical NDE Approach	148
6.1.3	A Numerical NDE Approach	149
6.1.4	A Numerical Study to Investigate the Possibility of Increasing PEC Sensor Resolution	149
6.2	Discussion of Limitations	150
6.3	Future Work	152
	Appendices	153
A	Analytical Approach: Interpreted Pipe Wall Thickness Maps and Error Statistics	155
B	Numerical and Probabilistic Approach: Interpreted Pipe Wall Thickness Maps and Error Statistics	167
C	On Site Pipe Scanning Protocol	179
D	Steps for Deriving the Eddy Current Diffusion Time Constant	181

Bibliography	183
---------------------	------------

List of Figures

1.1	PEC NDE: (a) PEC signal acquisition on an in situ critical pipe; (b) The commercial PEC sensor modeled in this thesis.	2
2.1	Basic setup of conventional EC inspection (Adapted from [1]).	18
2.2	Cross-sectional view of the typical detector coil based PEC sensor architecture used for ferromagnetic material thickness estimation.	22
2.3	Cross-sectional view of the typical detector coil based PEC sensor architecture used for pipe thickness assessment (The figure is not drawn to scale).	23
2.4	Cross-sectional view of the typical non-detector coil based PEC sensor architecture.	24
2.5	Detector coil based PEC signals processed in [2], acquired on Q235 steel: (a) Signals before filtering; (b) Signals after filtering	27
2.6	Detector coil based PEC signals processed in [3], acquired on Q235 steel: (a) Signals before processing; (b) Signals after processing	29
3.1	Mutually coupled coil architecture for PEC sensor modeling: (a) Mutually coupled coil model; (b) equivalent circuit model for pulsed eddy current testing system. (adapted from [4]).	38
3.2	Simultaneous differential equations governing the mutually coupled coil model (adapted from [4]).	39
3.3	PEC sensing unit used for the work of this thesis: (a) HSK 300 commercial PEC signal capturing unit; (b) 50 mm sensor used for this work (adapted from [5]).	44
3.4	Typical shape of a PEC signal produced by the HSK 300 unit (Captured on a 30 mm thick gray cast iron calibration block).	45
3.5	Decaying part of raw PEC signals for Mild Steel	46
3.6	Behavior of decay rate β against time for different thicknesses of Mild Steel.	47
3.7	Decaying part of raw PEC signals for Ductile Cast Iron.	48
3.8	Decaying part of raw PEC signals for Gray Cast Iron.	49
3.9	Behavior of $\beta(t)$ against $\ln[V(t)]$ of Mild Steel thicknesses from 1 mm to 12 mm, linearity observable between $\ln[V(t)] = 0$ and $\ln[V(t)] = 2$	50
3.10	Slight change in gradient as a signal enters the noise margin.	50
3.11	A fitted linear model to a noisy signal captured on gray cast iron.	52
3.12	Linear relationship between $\ln \beta_{max}$ and $\ln d$ for different ferromagnetic materials.	53
3.13	Low dependence on sensor lift-off.	56

3.14	Low dependence on sensor lift-off (Low Thicknesses).	56
3.15	Low dependence on sensor lift-off (High Thicknesses).	57
3.16	Impact of lift-off on the PEC signal for a fixed material thickness (Captured on a gray cast iron calibration block, 16 mm thickness).	59
3.17	Low dependence on sensor lift-off when the feature is considered in the form of $\ln \beta_{max}$	59
3.18	The two different PEC sensor sizes used for the experiment.	60
3.19	Variation of $\ln \beta_{max}$ values of two PEC sensor sizes against $\ln d$ for different thicknesses of gray cast iron.	61
3.20	Variation of absolute difference of feature values produced by the two sensor sizes against $\ln d$	61
3.21	Two sample curves produced by the two sensor sizes on a 10 mm gray cast iron calibration block.	62
3.22	Numerical PEC sensor simulation model: (a) 3D model of the sensor and pipe, (b) Cross-section showing induced fields.	63
3.23	Simulated sensor responses against unfiltered experimental signals for a range of gray cast iron thicknesses.	64
3.24	Effect of curvature on β_{max} for different thicknesses of gray cast iron.	64
3.25	Analytical model estimation.	66
3.26	Analytical model being used for critical pipe NDE.	68
3.27	Obtaining ground truth (GT).	69
3.28	Interpreted thickness map and GT for the first Gray Cast Iron pipe segment.	70
3.29	Interpreted thickness map and GT for the second Gray Cast Iron pipe segment.	71
3.30	Variation of interpretations along with GT for the Gray Cast Iron pipe segments.	71
3.31	Interpreted thickness map and GT for the Ductile Cast Iron pipe segment.	72
3.32	Variation of interpretations along with GT for the Ductile Cast Iron pipe segment.	72
3.33	Measuring pipe wall thickness using ultrasounds after cleaning the surface: (a) Ultrasound probe on pipe, (b) An ultrasound waveform.	74
3.34	Plot of $\ln \beta_{max}$ values for data obtained on a gray cast iron pipe segment.	75
3.35	Interpreted thickness map (by estimating c using ultrasounds) and GT for a Gray Cast Iron pipe segment.	75
3.36	Variation of interpretations (by estimating c using ultrasounds) along with GT for a Gray Cast Iron pipe segment.	76
3.37	Nonlinearity in the thickness-feature function in the low and high thickness ends for gray cast iron.	77
3.38	Variation of c of each measurement against $\ln d$ for gray cast iron.	77
3.39	Nonlinear variation of d against β_{max}	79
3.40	Graphical depiction of sensor noise characteristic when used on gray cast iron.	81
4.1	Steps for measuring electrical and magnetic properties of critical pipe materials. (Images adapted from http://www.diytrade.com/ and http://www.qdusa.com/)	85
4.2	Extracted specimens for testing material properties.	86

4.3	A magnetization curve measured from a specimen taken from a gray cast iron pipe segment.	87
4.4	In situ application of an XRF device for material analysis. (Image from http://www.electronicproducts.com/)	89
4.5	Temperature variation of electrical conductivity of gray cast iron pipe material (measured using Four Probe Method (PPMS)).	89
4.6	Microscopic view of micro-structures of cast irons: (a) Gray cast iron; (b) Nodular or Ductile cast iron.	90
4.7	Procedure followed to numerically simulate sensor signals.	91
4.8	Developed FEA model: (a) Complete model; (b) Zoomed view of the sensor.	96
4.9	Meshed FEA model: (a) Complete model; (b) Fine mesh of the sensor.	96
4.10	Cross-sectional view of the numerical model showing the eddy current induction phenomenon (Adapted from [6]).	97
4.11	Geometric properties of the excitation coil: (a) Plan view; (b) Side view.	98
4.12	Geometric properties of the detector coil: (a) Plan view; (b) Side view.	99
4.13	Numerically simulated PEC signals along with experiments (gray cast iron).	101
4.14	Feature values (β_{max}) vs thickness (d), agreement between simulation and experiments.	101
4.15	Correlation between the numerical simulation model and experiments.	102
4.16	Error between model and experiments against thickness.	102
4.17	Feature values ($\ln \beta_{max}$) vs thickness ($\ln d$), agreement between simulation and experiments.	103
4.18	Correlation between the numerical simulation model and experiments in terms of means of $\ln \beta_{max}$	104
4.19	Error between model and experiments against thickness for $\ln \beta_{max}$	104
4.20	Non-parametric learning of the thickness-feature function using GP.	105
4.21	Nonlinear thickness-feature function, <i>i.e.</i> , d vs β_{max} intended to be learned using GP, as described by simulated training data and experimental data.	108
4.22	Variation of negative log marginal likelihood against iteration number while optimizing GP model hyper-parameters starting from the initial condition $\theta^{(ini)} = [50, 0.7, 2]^T$	109
4.23	GP model being used for critical pipe NDE.	111
4.24	The GP model: Capturing nonlinearity in the low thickness range ($d \leq 5$ mm).	112
4.25	The GP model: Capturing nonlinearity for higher thicknesses ($d > 5$ mm)	112
4.26	GP interpreted thickness map and GT for the first Gray Cast Iron pipe segment.	113
4.27	GP interpreted thickness map and GT for the second Gray Cast Iron pipe segment.	113
4.28	Variation of GP interpretations and uncertainty along with GT for the Gray Cast Iron pipe segments.	114
5.1	2D Axisymmetric FEA model developed for the study: (a) 2D axisymmetric model; (b) Meshed model.	124

5.2	Feature values ($\ln \beta_{max}$) vs thickness ($\ln d$), agreement between simulation and theory.	127
5.3	Error between simulation and theory against thickness.	127
5.4	Correlation between the numerical simulation model and theory.	128
5.5	Numerically simulated signals by the 2D axisymmetric model for different thicknesses.	128
5.6	Induced eddy current density in a 25 mm thick plate displayed by the 2D axisymmetric model at a certain time instance.	129
5.7	Example for the impact of circular shape on the signal when comparing with the signal captured from the rectangular sensor (captured on a gray cast iron calibration block, 16 mm thickness).	132
5.8	Vertical domain of influence (penetration depth) of the base model.	133
5.9	Simulation model to investigate lateral domain of influence.	134
5.10	Lateral domain of influence.	135
5.11	Results from experiments done to increase sensor resolution.	137
5.12	Domain of influence of the small sensor with larger detector coil and increased excitation.	138
5.13	Thickness-feature function of the optimized sensor.	139
5.14	FEA model used for solving the problem of inferring thickness of both the healthy material layer and the top layer.	140
5.15	Influence on the signal caused by σ_t	141
5.16	Influence on the signal caused by σ_b	142
5.17	Thickness-feature function learned for the optimized circular sensor.	144
5.18	Learned function between lift-off and zero crossing time for $d = 10$ mm.	145
A.1	Analytical approach; Section 1; interpreted thickness and GT maps.	155
A.2	Analytical approach; Section 1; variation of interpreted thickness along with GT.	156
A.3	Analytical approach; Section 2; interpreted thickness and GT maps.	156
A.4	Analytical approach; Section 2; variation of interpreted thickness along with GT.	157
A.5	Analytical approach; Section 3; interpreted thickness and GT maps.	157
A.6	Analytical approach; Section 3; variation of interpreted thickness along with GT.	158
A.7	Analytical approach; Section 4; interpreted thickness and GT maps.	158
A.8	Analytical approach; Section 4; variation of interpreted thickness along with GT.	159
A.9	Analytical approach; Section 5; interpreted thickness and GT maps.	159
A.10	Analytical approach; Section 5; variation of interpreted thickness along with GT.	160
A.11	Analytical approach; Section 6; interpreted thickness and GT maps.	160
A.12	Analytical approach; Section 6; variation of interpreted thickness along with GT.	161
A.13	Analytical approach; Section 7; interpreted thickness and GT maps.	162

A.14 Analytical approach; Section 7; variation of interpreted thickness along with GT.	162
A.15 Analytical approach; Section 8; interpreted thickness and GT maps.	163
A.16 Analytical approach; Section 8; variation of interpreted thickness along with GT.	163
A.17 Analytical approach; Section 9; interpreted thickness and GT maps.	164
A.18 Analytical approach; Section 9; variation of interpreted thickness along with GT.	164
B.1 Numerical and probabilistic approach; Section 1; interpreted thickness and GT maps.	167
B.2 Numerical and probabilistic approach; Section 1; variation of interpreted thickness along with GT.	168
B.3 Numerical and probabilistic approach; Section 2; interpreted thickness and GT maps.	168
B.4 Numerical and probabilistic approach; Section 2; variation of interpreted thickness along with GT.	169
B.5 Numerical and probabilistic approach; Section 3; interpreted thickness and GT maps.	169
B.6 Numerical and probabilistic approach; Section 3; variation of interpreted thickness along with GT.	170
B.7 Numerical and probabilistic approach; Section 4; interpreted thickness and GT maps.	170
B.8 Numerical and probabilistic approach; Section 4; variation of interpreted thickness along with GT.	171
B.9 Numerical and probabilistic approach; Section 5; interpreted thickness and GT maps.	171
B.10 Numerical and probabilistic approach; Section 5; variation of interpreted thickness along with GT.	172
B.11 Numerical and probabilistic approach; Section 6; interpreted thickness and GT maps.	172
B.12 Numerical and probabilistic approach; Section 6; variation of interpreted thickness along with GT.	173
B.13 Numerical and probabilistic approach; Section 7; interpreted thickness and GT maps.	174
B.14 Numerical and probabilistic approach; Section 7; variation of interpreted thickness along with GT.	174
B.15 Numerical and probabilistic approach; Section 8; interpreted thickness and GT maps.	175
B.16 Numerical and probabilistic approach; Section 8; variation of interpreted thickness along with GT.	175
B.17 Numerical and probabilistic approach; Section 9; interpreted thickness and GT maps.	176
B.18 Numerical and probabilistic approach; Section 9; variation of interpreted thickness along with GT.	176

C.1	Placement of the grid and the sensor: (a) Grid wrapped around the pipe; (b) Sensor alignment.	179
C.2	How axial and circumferential directions of 2.5D thickness maps are located on a pipe: (a) Directions denoted on a 2.5D thickness map; (b) A rolled thickness map resembling a pipe; (c) How axial (x) and circumferential (y) directions appear on a pipe.	180

List of Tables

2.1	Summary of advantages and disadvantages of the application specific signal noise suppression techniques in relation to the target application of this thesis.	30
2.2	Aspects associated with previously proposed feature extraction techniques which limit their applicability for the work of this thesis.	33
3.1	Ferromagnetic material calibration block thicknesses.	46
3.2	Parameters of fitted straight lines for $\ln \beta_{max}$ vs $\ln d$ variation of different materials.	54
3.3	Statistics of absolute error between interpreted pipe wall thickness maps and ground truth for Gray Cast Iron pipe segments.	70
3.4	Statistics of absolute error between interpreted pipe wall thickness map and ground truth for the Ductile Cast Iron pipe segment.	73
3.5	Statistics of absolute error between interpreted pipe wall thickness map (by estimating c using ultrasounds) and ground truth for a Gray Cast Iron pipe segment.	75
3.6	Noise characteristic of the PEC sensor used for in situ applications when used on gray cast iron.	80
4.1	Parameters required for simulation.	100
4.2	Statistics of absolute error between interpreted pipe wall thickness and ground truth for Gray Cast Iron pipe segments.	115
4.3	Comparison of absolute error statistics between analytical and numerical approaches.	115
4.4	Comparison of absolute error statistics between analytical and numerical approaches (using all evaluated pipe segments).	116
5.1	Parameters required for simulation.	124
5.2	Agreement between the 2D axisymmetric model and theory, theoretical and simulated $\ln \beta_{max}$ values for different thicknesses.	126
5.3	Parameters required for simulation.	129
5.4	Shape dependence of $\ln \beta_{max}$ values.	131
5.5	3D profiling capability on gray cast iron: Results.	145
A.1	Statistics of absolute error between interpreted pipe wall thickness and GT for Section 1.	156
A.2	Statistics of absolute error between interpreted pipe wall thickness and GT for Section 2.	157

A.3	Statistics of absolute error between interpreted pipe wall thickness and GT for Section 3.	158
A.4	Statistics of absolute error between interpreted pipe wall thickness and GT for Section 4.	159
A.5	Statistics of absolute error between interpreted pipe wall thickness and GT for Section 5.	160
A.6	Statistics of absolute error between interpreted pipe wall thickness and GT for Section 6.	161
A.7	Statistics of absolute error between interpreted pipe wall thickness and GT for Section 7.	163
A.8	Statistics of absolute error between interpreted pipe wall thickness and GT for Section 8.	164
A.9	Statistics of absolute error between interpreted pipe wall thickness and GT for Section 9.	165
B.1	Statistics of absolute error between interpreted pipe wall thickness and GT for Section 1.	168
B.2	Statistics of absolute error between interpreted pipe wall thickness and GT for Section 2.	169
B.3	Statistics of absolute error between interpreted pipe wall thickness and GT for Section 3.	170
B.4	Statistics of absolute error between interpreted pipe wall thickness and GT for Section 4.	171
B.5	Statistics of absolute error between interpreted pipe wall thickness and GT for Section 5.	172
B.6	Statistics of absolute error between interpreted pipe wall thickness and GT for Section 6.	173
B.7	Statistics of absolute error between interpreted pipe wall thickness and GT for Section 7.	175
B.8	Statistics of absolute error between interpreted pipe wall thickness and GT for Section 8.	176
B.9	Statistics of absolute error between interpreted pipe wall thickness and GT for Section 9.	177

Abbreviations

2.5D	Two and a half Dimensional
3D	Three Dimensional
EC	Eddy Current
EDM	Electrical Discharge Machining
FEA	Finite Element Analysis
GP	Gaussian Process
GT	Ground Truth
MFL	Magnetic Flux Leakage
NDE	Nondestructive Evaluation
PEC	Pulsed Eddy Current
PPMS	Physical Property Measurement System
RFT	Remote Field Testing
RMS	Root Mean Square
RSG	Rock Solid Group
SNR	Signal to Noise Ratio
SQUID	Superconducting Quantum Interference Device
UTS	University of Technology Sydney
XRF	X-Ray Fluorescence

Nomenclature

Symbol	Quantity
\vec{A}	Magnetic vector potential
\vec{B}	Magnetic flux density
\vec{D}	Displacement current
d	Thickness of the ferromagnetic material in meters
\vec{E}	Electric field intensity
f	Frequency
$f(\cdot)$	A scalar valued function
\vec{H}	Magnetic field intensity
\vec{J}	Electric current density
$K(\cdot, \cdot)$	Kernel
$n(t)$	Time varying noise
$P(\cdot)$	Probability
R	Correlation coefficient
\mathbb{R}^+	Set of positive real numbers
S	Numerically simulated PEC signal from the 3D sensor model
S_{2D}	Numerically simulated PEC signal from the 2D axisymmetric sensor model
T	Absolute temperature
t	time
t_{th}	Threshold crossing time for lift-off quantification
$V(t)$	Noise free induced detector coil voltage in time domain
$V_e(t)$	Noisy induced detector coil voltage such that $V_e(t) = V(t) + n(t)$

X	Set of training inputs for GP
X^*	Set of testing inputs for GP
Y	Set of training targets for GP
$\beta(t)$	Decay rate in time domain
β_{max}	Decay rate feature for thickness quantification
ϵ_0	Permittivity of free space (8.854×10^{-12} F/m)
ϵ_{noise}	Uncertainty encapsulating noise
θ	Set of hyper-parameters for GP
μ	Permeability ($\mu_r \mu_0$)
μ_0	Permeability of free space ($4\pi \times 10^{-7}$ H/m)
μ_m	Mean function for GP
μ_m^*	GP estimate (mean of posterior distribution)
μ_r	Relative permeability
Σ	Covariance function for GP
Σ_{un}^*	Estimated uncertainty for GP estimates
σ	Electrical conductivity
Φ	Magnetic scalar potential

Glossary of Terms

Autonomous	Without human intervention.
Calibration Blocks	Cuboid shaped blocks fabricated from desired materials to known dimensions for the purpose of calibrating EC/PEC sensor readings.
Critical Pipes	Large diameter (usually $\geq 300\text{mm}$) high pressure pipes owned and managed by water utilities to distribute consumable fresh water to customers.
Critical Pipe Materials	Materials usually used for manufacturing critical pipes (gray cast iron, ductile cast iron and mild steel).
Lift-off	Vertical distance between an EC/PEC sensor and the surface of the test piece being evaluated
Training Data	Data used in various areas of information science to discover potentially predictive relationships.

Chapter 1

Introduction

Modern day maintenance of civil infrastructure demands significant attention to structural health monitoring. The fact that assessment of surface condition alone being insufficient for health and strength assessment of most solid structures, creates the necessity to evaluate the integrity of subsurface regions. Though condition assessment via accessing subsurface regions using solid state sensors is not possible, and destructively reaching subsurface regions is not desired, state of the art sensors have been developed to enable Nondestructive Evaluation (NDE) by means of induced fields and reflected waves. Such NDE techniques have evolved over the past five decades and are widely being used in different industries at present for condition assessment of civil infrastructure [7].

This thesis focuses on approaches for solving the problem of acquiring and representing the geometry of electrically conductive ferromagnetic materials via Pulsed Eddy Current (PEC) sensor based NDE. The target application is condition assessment of critical pipes; *i.e.*, large diameter (usually ≥ 300 mm) high pressure pipes owned and managed by water utilities to distribute consumable fresh water to customers. Critical pipes are manufactured from gray cast iron, ductile cast iron and mild steels. Therefore, critical pipe materials are conductive and ferromagnetic in nature.

Analytical and numerical approaches are developed in the thesis for NDE via modeling PEC sensor interaction with conductive ferromagnetic materials in order to study, characterize and quantify effects of material geometry on sensor signals. The objective is to use

sensor models to characterize relationships between signals and material geometry, and use the characterized relationships to interpret real world PEC signals for ferromagnetic material specific quantitative condition assessment purposes.

The thesis presents: (a) a novel PEC signal feature possessing a useful representative capability of test piece geometry, and analytically described fundamentals behind the feature's behavior; (b) an experimental+analytical approach which exploits the feature to perform NDE of critical pipes; (c) a numerical+probabilistic approach which exploits the feature to perform NDE of critical pipes; and (d) a study on optimizing sensor geometry to achieve higher resolution while maintaining measurement capabilities suitable for critical pipe assessment. NDE related outcomes of the thesis are evaluated by applying them for in situ critical pipe condition assessment (Fig. 1.1), and validating interpreted pipe conditions against destructively measured actuality. Though sensor modeling approaches presented in this thesis generalize, they are specifically evaluated through using them to model a commercial PEC sensor provided by Rock Solid Group[©] (RSG) (<http://www.rocksolidgroup.com.au/>).

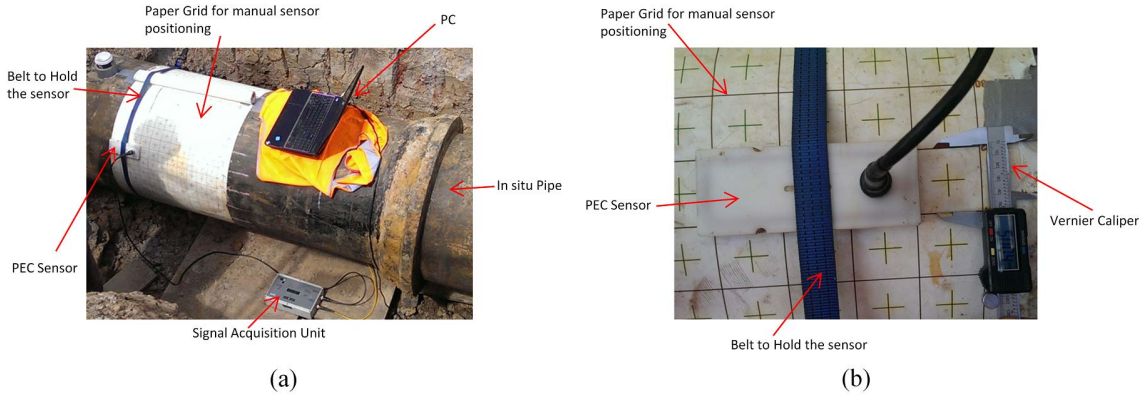


FIGURE 1.1: PEC NDE: (a) PEC signal acquisition on an in situ critical pipe; (b) The commercial PEC sensor modeled in this thesis.

This chapter introduces the research work presented in the thesis. It commences with a background of the target application scenario of critical pipe evaluation and details key research issues. The remaining sections of this chapter describe the thesis scope and its main contributions and provide the outline of the remainder of the thesis.

1.1 Background

It is generally recognized worldwide that about 70% of the total asset base of urban water utilities consists of buried pipes [8]. Sydney Water (<http://www.sydneywater.com.au/>) has buried systems valued at over AU\$15 billion and this is typical of large utilities.

Most major urban water utilities in Australia have extensive large, critical pressure main systems, parts of which have been in service up to a century or more [8–10]. Failure of critical pipes has significant impact on maintaining service levels to customers, loss of fire fighting supply, compromised safety, transport disruption and other social costs, as well as significant financial and reputational implications.

With further aging of this vital infrastructure, critical pipe failures will continue to occur. This will have very high and growing cost implications for the sustainability and effectiveness of water and wastewater services. This is a worldwide issue, with potential impacts of climate change on soil properties and moisture which lead to higher costs.

In Australia, the total replacement costs of the pipe network have been estimated to exceed AU\$100 billion [10]. Over the next five years, the costs of urgently needed asset replacement are around AU\$5 billion. Maintenance costs over the same period are estimated at some AU\$2.5 billion [10]. Elsewhere, the USEPA estimates that the US public water sector will require US\$335 billion of capital investment over the next 20 years to sustain essential service levels. Also, US studies indicate that the average cost per failure for large diameter pipes exceeds US\$500,000 [10].

In response to these cost drivers, and to meet demands for reliable water supply services, water utilities have already made considerable efforts to control potential failures by applying existing, state-of-the-art methods for failure prediction, condition assessment and proactive pipe asset management technologies. The methods used have limited level of confidence which limits the ability to target renewal programs. It has been conservatively estimated that even a 30% improvement in the present state of the art, would reduce the high consequence events by 50% and total failure events by 30% resulting in potential savings of over AU\$160 million over a 20 year period to the Australian Water industry [10]. With better prediction from condition assessment, expenditure can be delayed by

5 years and replacement costs reduced up to 20%, the projected savings over a 20 year period will exceed a further AU\$300 million [10].

Water utilities urgently need better techniques for estimating the probability of failure of critical pipelines and for estimating their remaining life. The unavailability of such tools increases the risk of substantial funds being potentially misdirected through premature replacements. This could impact on future water service pricing. On the other hand, not undertaking timely replacement of pipes could lead to increasing number and frequency of failures with associated costs and disruption.

Corrosion and graphitization are the main causes which weaken the strength of aging critical pipes and cause them to fail eventually [8, 11]. Knowing the amount of non-compromised conductive ferromagnetic material remaining in pipe walls is therefore the key first step towards lifetime or failure prediction. Since corrosion and graphitization occur on inner and outer surfaces of pipe walls, healthy material often remain in subsurface regions which cannot be accessed directly. Causing any physical destruction to critical pipes even in the form of corrosion removal done to access the healthy material surface is undesired due to the risk of pipe bursts. Therefore, the amount of healthy material can only be evaluated nondestructively. Consequentially, many NDE techniques have emerged and grown in demand in the field of critical pipe condition assessment [12].

Due to the conductive and ferromagnetic nature of critical pipe materials, electromagnetic NDE techniques such as PEC (the focus of this thesis), Magnetic Flux Leakage (MFL) and Remote Field Testing (RFT) are widely used for critical pipe condition assessment [12]. Though these technologies are well established and provided commercially at present, the techniques used in practice have shortcomings. One issue is the requirement of sensor calibration to achieve quantitative interpretation of pipe condition [6, 13, 14]. Accurate calibration is challenging in the target application due to the difficulty of obtaining calibration materials having properties which satisfactorily match those of critical pipes. As a result of calibration errors, interpreted pipe conditions can be observed to deviate from reality in practice. Another issue is the requirement of time intensive manual labor to analyze signals individually to accomplish accurate interpretation. Although ferromagnetic material specific PEC signal processing techniques have been proposed [4, 13, 14],

an autonomous framework which is readily usable with a commercial PEC tool is lacking. A system which models sensors taking into account unknown material properties and hence autonomously inferring pipe condition using NDE data, has the potential to greatly increase productivity of the process and the accuracy of results.

This thesis originated as a part of Activity 2 of the Advanced Condition Assessment & Pipe Failure Prediction Project (<http://www.criticalpipes.com/>), which is co-led by University of Technology Sydney (UTS). The project is strongly supported by Sydney Water and many Australian and international water utilities, condition assessment service providers and research institutions. This activity aims to advance knowledge and improve levels of confidence of direct methods for condition assessment using sensor modeling and advanced data interpretation techniques which have already been successfully employed in fields such as aerospace, cargo handling, undersea ecology, land vehicles and mining. The desired outcome of Activity 2 is a method of accurately predicting sensor readings for a given geometric description of a buried large critical pipe, and obtaining the best estimate of the pipe geometry from a set of measurements based on maximum likelihood principles. As a part of this activity, this thesis deals with PEC sensor specific modeling and data interpretation.

1.2 Motivation

PEC sensor signals are strictly dependent on the geometry and electrical and magnetic properties of the material being tested. Therefore, to ensure accurate assessment of geometric condition of a certain material, sensor readings require to be calibrated with respect to material geometry. Common industrial practice of PEC sensor calibration with respect to geometry involves using readings acquired on reference test pieces with known geometry and intrinsic material properties as close as possible to those of the actual material being evaluated. Such reference test pieces used for calibration are henceforth referred to as “calibration blocks” in this thesis.

Calibration blocks can be either fabricated or destructively extracted from the domain being evaluated. In the application of critical pipe evaluation however, destructive extraction is not possible due the physical damage it causes to the infrastructure. As a result, common industrial practice enables geometric calibration of critical pipe materials only by means of fabricated calibration blocks.

To fabricate calibration blocks which replicate the desired geometric sensitivity, precise intrinsic properties (specifically electrical conductivity and magnetic permeability) of the material to be evaluated have to be known. That enables fabricating calibration blocks having identical or at least very close, intrinsic properties to those of the material required to be tested. When it comes to pipe assessment however, precise intrinsic properties of pipe materials are unknown. Specifically, the pipes in focus of this thesis were manufactured and laid in the early 19th century where quality control methods were not widely enforced. Though measuring the necessary properties is a possibility, having the capability to manufacture a critical pipe material to have the exact measured intrinsic property values is highly unlikely. This is due to critical pipe materials being manufactured by casting and cooling, a process highly influential on intrinsic properties of the end product. Expecting a casting and cooling process to repeat itself identically, so that the exact properties of a previously manufactured material sample is replicated, is highly ambitious. Further, fabricating tailored calibration blocks on each condition assessment undertaken is undesired due to the cost, time and labor requirement constraints.

Usual practice followed by commercial PEC service providers to avoid the aforementioned constraints is performing one off fabrication of sets of calibration blocks. Such a method is reasonable for materials which can be guaranteed to have fairly precise intrinsic properties and narrow margins of variation. In light of critical pipe materials however, that is not the case. For critical pipe materials which include gray cast iron, ductile cast iron and mild steel, electrical conductivity and magnetic permeability values can vary approximately up to $\pm 20\%$ from the expected mean [15]. Reasons behind such a variation are the high degree of inhomogeneity in the materials itself, and the nonlinearity attributed with intrinsic properties [15]. Therefore, electrical and magnetic properties of critical pipe material specific calibration blocks could deviate within $\pm 20\%$ from those of pipes. Such discrepancies between calibration and measurement adversely affect the measuring technique by

offsetting interpreted geometric condition from reality.

Another issue related to the NDE techniques, especially the commercially provided ones, is the requirement of time intensive manual labor to analyze signals individually to accomplish accurate interpretation. The lack of efficient algorithms to autonomously interpret data negatively impact service providers by hampering their delivery speed of results. Although ferromagnetic material specific PEC signal processing techniques have been proposed [4, 13, 14], autonomous data interpretation frameworks which are readily usable with commercial PEC tools to make them more efficient are not common.

Developing methods of taking into account measured electrical and magnetic properties of materials and artificially generating NDE signals via computational means to eliminate the requirement of calibration blocks are clearly warranted. Approaches which use calibration data to learn relationships between signal features and material geometry are also necessary to enable efficient and autonomous interpretation of signals.

1.3 Scope

The thesis specifically aims to develop PEC based advanced NDE approaches suitable for critical pipe condition assessment. Developed approaches are intended to overcome the issues related to calibration and requirement of manual data interpretation, in addition to being able to accurately predict pipe condition with confidence bounds. Two approaches are developed with the objective to learn functions which map PEC signal features to test piece geometry and use the learned functions to interpret PEC data acquired from on site measurements to predict geometric condition of in situ critical pipes.

It should be noted that designing a novel PEC sensor architecture to produce more accurate measurement capabilities is beyond the scope of this research. The objective is to rather use a standard PEC sensor architecture which is used by RSG, the commercial PEC service provider partnering with this research, and to propose approaches to better interpret the data. Therefore, the scope of this thesis is limited to the “detector coil” based PEC sensor architecture, which is the one used by RSG. All Eddy Current (EC) and PEC sensors operate by a coil (exciter coil) being excited by a time varying current which induces eddy

currents in the test piece, and using a receiver/detector to capture the resultant time varying magnetic field. Since the influence of eddy currents induced in the test piece are contained in the resultant magnetic field, the signal induced by the detected field can be used to characterize different properties of the test piece. Though all EC and PEC sensor architectures have an exciter coil in common, the sensor architectures differ based on the type of detector used [1].

The detector coil based PEC sensor architecture is known to have superior sensitivity to geometric properties of conductive ferromagnetic materials over other architectures [1], thereby making it the most suitable architecture for the target application. Subject to the capabilities of the used architecture, pipe geometry is evaluated and presented in the form of average wall thickness remaining under the detector coil. When a condition assessment is done, the thickness estimates are presented as a 2.5D thickness map which uses pipe axial and circumferential positions as x and y coordinates respectively to represent the location of each thickness estimate. Hence the scope of assessed pipe condition is limited to average wall thickness under the detector coil.

The target application of this thesis is critical pipe assessment, aged critical pipes are found in either of the three critical pipe materials: gray cast iron, ductile cast iron or mild steel [8, 9, 11]. Thus, all NDE related developments are experimented on in situ pipes made of critical pipe materials. However, the proposed approaches generalize for condition assessment of any electrically conductive and ferromagnetic material.

A novel PEC signal feature, the “detector coil voltage decay rate” is introduced in this thesis. Existence of a functional behavior between the feature and conductive ferromagnetic material thickness is theoretically proved and experimentally verified. Suitability of the feature for critical pipe condition assessment is demonstrated.

The thesis presents two NDE approaches based on the “detector coil voltage decay rate” signal feature. First, an analytical approach which requires experimental calibration and secondly a probabilistic approach which uses numerically modeled data for learning. In the first approach, calibration data are obtained from calibration blocks and a function between thickness and a signal feature is analytically derived using calibration data. This

function is eventually used to interpret NDE signals to predict thickness of in situ critical pipes. Accuracy of the pipe conditions interpreted by the approach is quantitatively evaluated. The method requires the aid of calibration blocks, or alternatively as proposed in this thesis, ultrasound measurements performed on pipe sections. Consequentially, the requirement of the probabilistic approach based on numerical modeling is proposed to eliminate the requirement of calibration and to capture nonlinearities. The second approach deals with experimentally measuring intrinsic electrical and magnetic properties of pipe materials, using the measured properties to numerically simulate PEC signals using a Finite Element Analysis (FEA) [16, 17] model and probabilistically learning the thickness-feature function. Gaussian Process (GP) [18] is used as the probabilistic approach to learn the nonlinear function since it yields the useful information of uncertainty for inferences performed. The hence learned function is used for in situ critical pipe assessment, the performance of the second approach is also evaluated.

Due to the fact that the PEC sensor architecture used for this work can measure only the average thickness which generalizes to a region underneath the sensor, sensor resolution is primarily limited by the sensor size. This limitation in resolution prevents identification and quantification of fine defects, identified as an additional research challenge. In the view of the constraints on altering the existing design, this thesis presents an FEA based study on optimizing the PEC sensor geometry to achieve better resolution while maintaining penetration and measurement capabilities required for in situ critical pipe assessment. In addition to increasing resolution, the thesis presents a framework applicable for 3D profiling by means of concurrent inference of material thickness and lift-off, the vertical distance between the sensor and the conducting material surface.

The thesis thus presents the theoretical fundamentals behind the detector coil voltage decay rate signal feature, a numerical study focused on optimizing sensor geometry to achieve better resolution facilitate 3D profiling capability and presents the critical pipe NDE approaches implemented as frameworks so that they generalize to any detector coil based PEC sensor.

1.4 Contributions

The contributions of this thesis are:

1. Introduction of a novel PEC signal feature based on the detector coil voltage decay rate as a feature capable of thickness discrimination of conductive ferromagnetic materials and the validation of the feature's monotonic functional behavior with thickness [19]. Fundamentals behind the feature's behavior are analytically described and experimentally validated, and suitability for critical pipe assessment is established.
2. An analytical approach to parametrically learn the thickness-feature function and use it for PEC NDE of critical pipes [19]. Function parameters are estimated for critical pipe materials via experiments performed on calibration blocks and the function's performance on in situ critical pipe assessment is evaluated. The practical difficulty of obtaining calibration blocks which have properties matching those of critical pipe materials substantiates the need for an alternative calibration method based on two sensing modalities; a method of calibrating by means of PEC and ultrasound measurements is proposed [19].
3. A critical pipe NDE approach which takes into account measured electrical and magnetic properties of critical pipe materials to simulate PEC sensor responses using FEA, and non-parametrically learns the thickness-feature function using the decay rate feature extracted from simulated sensor responses. Simulation is done using a validated FEA model [6] tailored to represent the commercial PEC sensor used for this work. Measured electrical and magnetic properties of critical pipe materials are incorporated with properties of the sensor, and the sensor's interaction with the material being tested is numerically modeled [6]. The modeling technique presented generalizes to model any EC/PEC sensor's interaction with a conductive material. Learning the thickness-feature function is done probabilistically using GP and the performance on in situ critical pipe assessment is evaluated against ground truth after destructive testing. Non-parametric probabilistic learning demonstrates increased accuracy over the analytical approach due to being able to learn and model local nonlinearities present in the thickness-feature function.

4. Low resolution associated with the commercial PEC sensor used for this work is identified as an additional limitation. A simulation study is carried out to optimize the sensor geometry with the objective of achieving better resolution while maintaining the desired penetration capability suitable for critical pipe assessment. The study also suggests a framework applicable for 3D profiling by quantifying material thickness and sensor lift-off concurrently.

1.5 Publications

The following peer reviewed research papers were either published during candidature or were being reviewed at the time of completion of this thesis. Some publications are not directly related to the work of the thesis, however, techniques presented in such publications are adapted and incorporated within the thesis. Notations 'J' and 'C' refer to journal articles and conference papers respectively.

1.5.1 Directly Related Publications

- J1. Jaime Valls Miro, Jeya Rajalingam, Teresa Vidal-Calleja, Freek de Bruijn, Roger Wood, Dammika Vitanage, **Nalika Ulapane**, Buddhi Wijerathna, and Daoblige Su, “A live test-bed for the advancement of condition assessment and failure prediction research on critical pipes,” *Water Asset Management International*, ISSN Print: 1814- 5434, ISSN Online: 1814-5442, 10(2):03-08, 2014.
- J2. **Nalika Ulapane**, Alen Alempijevic, Jaime Valls Miro, Teresa Vidal Calleja, “Non-destructive evaluation of ferromagnetic material thickness using Pulsed Eddy Current sensor detector coil voltage decay rate,” *NDT & E International*, 2014, Under Review.
- C1. **N. Ulapane**, A. Alempijevic, T. Vidal-Calleja, J. V. Miro, J. Rudd, and M. Roubal, “Gaussian process for interpreting pulsed eddy current signals for ferromagnetic pipe profiling,” in *Proceedings of the 9th IEEE International Conference on Industrial Electronics & Applications (ICIEA)*, pp. 1762-1767, 2014.

1.5.2 Indirectly Related Publications

- J3. **Nalika Ulapane**, Sunil Abeyratne, Prabath Binduhewa, Chamari Dhanapala, Shyama Wickramasinghe, Nimal Rathnayake, “A Simple Software Application for Simulating Commercially Available Solar Panels,” *International Journal of Soft Computing And Software Engineering (JSCSE)*, e-ISSN: 2251-7545, Vol.2,No.5, pp. 48-68, 2012
- C2. **Nalika N.B. Ulapane** and Sunil G. Abeyratne, “Gaussian process for learning solar panel maximum power point characteristics as functions of environmental conditions,” in *Proceedings of the 9th IEEE International Conference on Industrial Electronics & Applications (ICIEA)*, pp. 1756-1761, 2014.
- C3. Daobilige Su, **Nalika Ulapane** and Buddhi Wijerathna, “An acoustic sensor based novel method for 2D localization of a robot in a structured environment,” in *Proceedings of the 10th IEEE International Conference on Industrial Electronics & Applications (ICIEA)*, 2015, in press.

1.6 Thesis Layout

The thesis is structured so the first two chapters outline the research and provide background for the thesis. Chapter 3 introduces the detector coil voltage decay rate as a PEC signal feature suitable to evaluate conductive ferromagnetic material thickness and presents the decay rate based analytical approach for NDE of critical pipes. The requirement of accurate calibration in this approach leads to the realization why the numerical approach proposed in Chapter 4 is required. Chapter 4 presents the decay rate based numerical sensor modeling technique and the probabilistic thickness-feature function learning approach for NDE of critical pipes. Chapter 5 presents the study on optimizing sensor geometry to increase resolution and enable 3D profiling. Conclusions are presented in Chapter 6. The detailed outline of each chapter follows:

Chapter 2 contains a review of related work in the field of PEC sensing. The chapter presents PEC sensor operating principles, sensor architectures and applications. Further, the chapter investigates PEC signal features used in practice and their applications. PEC

sensor modeling techniques are subsequently investigated and the chapter concludes by reviewing already published knowledge on the influence of sensor geometry on measurement capabilities.

Chapter 3 introduces the detector coil voltage decay rate as a PEC signal feature suitable for conductive ferromagnetic material thickness discrimination. Analytical derivations result in a parametric function which maps the feature value to thickness. The functional behavior of the feature is demonstrated for pipe materials using experimental PEC signals obtained from calibration blocks. Some important low dependencies associated with the decay rate feature are hypothesized and experimentally validated. These low dependencies on certain factors make the feature immune to some practical anomalies encountered during performing in situ measurements. Since the target application is critical pipe evaluation, and the fact that pipe walls are curved unlike calibration blocks, the effect of test piece curvature on the feature is numerically studied using FEA determining a curvature range which does not impact significantly on the feature. The decay rate based analytical approach for NDE of critical pipes is also presented. Readings on calibration blocks are used to estimate parameters of the thickness-feature function for different pipe materials. The learned function is then used for wall thickness estimation of in situ critical pipes and the accuracy of results is demonstrated. To avoid requirement of calibration, an alternative method is introduced to estimate thickness by using ultrasound measurements for scaling. The chapter concludes by characterizing sensor noise and identifying the requirement of calibration as a practical difficulty which has to be adhered with when executing the proposed approach in addition to the limitation of the approach not being able to accurately model local nonlinearities present in the thickness-feature function.

Chapter 4 presents the numerical and probabilistic approach for NDE of critical pipes. Methods followed for measuring electrical and magnetic properties of in situ critical pipe materials are discussed. The development of the FEA model of the commercial PEC sensor used for this work is presented. The model is validated by comparing the simulations with experimental results obtained from a range of calibration blocks. Decay rate feature values are extracted from simulated sensor signals and are used as training data to non-parametrically learn the thickness-feature function using the probabilistic technique of GP. The hence learned function is validated on wall thickness estimation of in situ critical

pipes using feature values extracted from on site NDE measurements. This approach proves a slight superiority over the analytical approach due to being able to learn local nonlinearities in the thickness feature-function.

Chapter 5 identifies the low resolution associated with the commercial PEC sensor used for this work as an additional limitation. An FEA based simulation study is carried out to optimize the sensor geometry with the objective of achieving better resolution while maintaining the penetration capability required for critical pipe assessment. The chapter concludes by presenting a framework usable for 3D profiling by means of concurrently inferring material thickness and sensor lift-off.

Chapter 6 summarizes the research work presented in this thesis followed by a discussion on limitations of the decay rate feature, implemented NDE approaches and the sensor optimization study. Conclusions are drawn with regards to this research and avenues for future work are proposed.

Chapter 2

Review of Related Work

There are numerous challenges in developing an NDE approach which takes into account measured intrinsic properties of a material, models sensor signals to learn functions between signal features and material geometry, and eventually use the function to autonomously interpret signals acquired from on site NDE measurements to predict test piece geometric condition. Since the target application is clearly defined to be critical pipe wall thickness evaluation and the scope is limited to using PEC sensors, the main research challenges involved are: (a) Identifying a suitable sensor architecture; (b) Sensor modeling; and (c) Identifying thickness discriminative signal features.

PEC technique is a category of EC inspection techniques and the justification behind selecting the PEC technique for the target application over other EC techniques has to be clearly understood. This chapter therefore begins by reviewing the available EC inspection techniques and their capabilities and limitations so that the reason behind choosing the PEC technique is clarified.

Though there are a few different PEC sensor architectures, the detector coil based architecture is the one used for the work of this thesis. This architecture had to be incorporated mainly due to the commercial sensor partnering with this work being based on it. However, this architecture is also the most suitable and the most commonly used one for ferromagnetic material thickness quantification. After reviewing EC inspection techniques, this

chapter reviews the PEC sensor architectures to help understand the suitability of the detector coil based architecture for the target application of this thesis.

Subsequently, existing work on PEC based ferromagnetic material thickness quantification are reviewed. This mainly highlights application specific signal noise suppression and thickness discriminative feature extraction techniques which have been previously proposed. Suitable noise suppression techniques presented in literature are adapted and used for signal processing in this thesis. However, the review on thickness discriminative features helps to realize their characteristics which make them not ideal for the target application of critical pipe evaluation. This brings to the realization about why the newly proposed PEC signal feature in this thesis, the “detector coil voltage decay rate” is required.

Finally, the chapter reviews previous studies on the influence of sensor geometry on measuring capabilities. This thesis eventually builds on that knowledge to study the possibility of increasing PEC sensor resolution with respect to the target application. The chapter concludes with a summary of findings so that the research gaps this thesis attempts to fill become clear.

2.1 EC Inspection Techniques

EC inspection techniques can mainly be classified into (a) single frequency EC techniques and (b) multi-frequency EC techniques [1]. The conventional EC techniques fall into the single frequency EC class whereas PEC falls into the multi-frequency class [1]. However, due to its quick excitation and small excitation time, the PEC technique stands out from the class of multi-frequency techniques. Therefore, the single frequency EC technique, the multi-frequency EC technique and the PEC technique are addressed separately in subsections 2.1.2, 2.1.3 and 2.1.4 respectively. Remote Field Eddy Current Testing (RFT) is another important derivative of EC inspection [1, 20]. RFT is very useful when inspecting large test pieces such as water, oil and gas pipelines due to its sensor architecture and the operating mechanism which enables it to examine large areas in a short space of time [1, 20]. However, RFT is not considered as a separate EC technique in this review since

its operating principle is based on single frequency and multi-frequency EC principles despite the sensor architecture being different. Therefore, RFT technique is not addressed in length in this review.

The operating principle of all EC techniques is the same and before elaborating on different EC inspection techniques, EC sensor operating principles are briefly explained in subsection 2.1.1 while formula based detailed theoretical descriptions are provided in Chapters 3 and 4.

2.1.1 Principle of EC Inspection

The principle of eddy current inspection is based on the interaction between a magnetic field source and a test material. This interaction induces eddy currents in the test piece and the presence of cracks or other imperfections can be detected by monitoring changes in the eddy current flow [21]. According to Ampere's law, when a time varying current passes through a conductor, a resulting time varying magnetic field is generated around it. When such a conductor is placed adjacent to another conducting material, eddy currents are induced in the conducting material in accordance with Faraday's and Lenz's laws. The eddy currents propagate in circular paths and eddy current densities are sensitive to properties of the conductive material in which the eddy currents are flowing. Some examples of these properties are: material conductivity, material composition, magnetic permeability, stress and strain, temperature, material volume and flaws in the material [1]. Thus, if the variations occurring in the induced eddy currents are sensed and quantified, it is possible to estimate the aforesaid material properties [1].

2.1.2 Conventional (Single Frequency) EC Inspection

The single frequency conventional eddy current inspection technique is the most preliminary of all the EC techniques and was the first EC testing method to be evolved more than half a century ago [1, 22]. When coil probes are used, this technique is usually operated as per Fig. 2.1. A single exciter coil is placed above a test piece and the coil is excited by a sinusoidal input with a certain frequency. The excited coil would have defined impedance

when standing alone. However, when it is placed above a test piece, eddy currents are induced in the test piece and this causes a change in the impedance of the coil due to magnetic field interaction. The impedance change is affected by the eddy currents inducing a reverse electromotive force on the coil. This change in impedance can then be plotted on a normalized impedance plane modeled to extract properties of the test piece [1, 22–25].

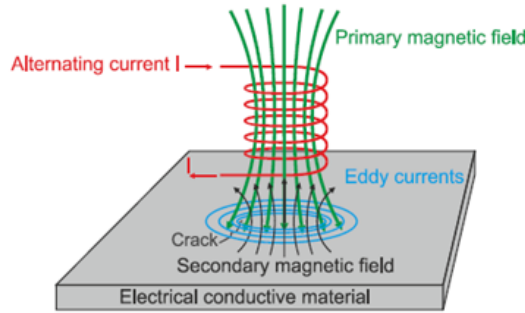


FIGURE 2.1: Basic setup of conventional EC inspection (Adapted from [1]).

A major drawback in the conventional EC inspection technique is the skin effect limitation [1]. It is known that the depth of penetration of the eddy currents is inversely proportional to the square roots of: (a) Electrical conductivity of the material; (b) Magnetic permeability of the material; and (c) The frequency of the excitation voltage. Since critical pipe materials are conductive and ferromagnetic, they usually have high conductivity and permeability values. Therefore, for a given frequency, eddy current penetration depth in these materials will be lower than a nonmagnetic material having similar conductivity. As a result, the conventional EC technique is typically used for crack/defect identification in nonmagnetic materials [23–25], in applications such as aircraft inspection [23, 24]. Furthermore, it is known that despite this technique being capable of assessing geometric condition of nonmagnetic materials, it does not have the same capability when assessing ferromagnetic materials [1]. The reason for this is the sensor’s sensitivity to test piece geometry being overshadowed by its sensitivity to material permeability due to the permeability of ferromagnetic materials being high. Therefore, the conventional EC technique can be used to easily discriminate ferromagnetic materials from nonmagnetic materials [1] and it can be effectively used for quantifying material properties such as magnetic permeability as done in [26]. However, the sensor’s sensitivity to the geometry of ferromagnetic

materials is minimal and as a result, the conventional EC technique is not suitable for the target application of critical pipe assessment.

Multi-frequency techniques were developed to overcome the skin effect limitation associated with the conventional technique.

2.1.3 Multi-Frequency EC Inspection

Multi frequency techniques use a combination of several excitation signals with several frequencies; different frequencies penetrate different depths and provide information about different locations on the test piece [1]. Therefore, the multi-frequency technique can handle the skin effect limitation better than the conventional technique while being able to provide more information at different depths [1].

Given the inverse relationship between eddy current penetration depth and frequency, it can be hypothesized that higher penetration depth can be achieved by exciting with lower frequencies, and therefore, a multi-frequency technique can assess any depth of any material including ones having ferromagnetic properties. Though achieving higher penetration in such a way is fundamentally possible, a hence achieved penetration is hardly usable for condition assessment due to the reason detailed henceforth. Nondestructive condition assessment of electrically conductive materials when using electromagnetic sensors can be done only by reading the magnetic field resulting from excitation fields interacting with the test piece. Such a resultant magnetic field has the frequency of the excitation signal and the field can be read by measuring a current or a voltage induced by it. Since induction follows Faraday's law, the magnitude of induced fields are proportional to the rate of change of magnetic flux, *i.e.*, the frequency of the magnetic field. Consequentially, lower frequencies will result in lower induced fields which can be difficult to measure, despite they cause eddy currents to penetrate deeper. As a result, using multiple excitation frequencies, or simply using lower excitation frequencies is not an ideal option for conductive ferromagnetic material inspection. Therefore, multi-frequency techniques too are generally used for assessing nonmagnetic materials [27–29]. Although the multi-frequency technique too in its usual form is not suitable for geometric condition assessment of ferromagnetic materials, exploiting it in the form of the PEC variant produces some salient

properties which are greatly advantageous and create the desired geometric sensitivity when interacting with ferromagnetic materials.

2.1.4 PEC Inspection

The main difference of the PEC technique is the sensor being excited by a voltage or a current pulse as opposed to being excited by a set of frequencies as in multi-frequency techniques. This technique stands out as the most versatile and modern counterpart of EC techniques at present [1].

PEC technique has proven itself to be able to easily overcome the skin effect and produce detectable magnetic field variations at the same time due to the salient characteristics of its pulsed excitation. It has therefore commonly been used for geometric condition assessment of ferromagnetic materials in the recent past [2–4, 6, 13, 14, 19, 20, 30–33].

Rising and falling edges of the pulsed excitation can be theoretically described by a Heaviside step function. The Fourier transform of the Heaviside function is known to be $\delta(f) + \frac{1}{i2\pi f}$ where $i = \sqrt{-1}$, f denotes frequency and $\delta(f)$ denotes the unit impulse function of f . This result clearly suggests that the power of low frequencies can be very high. A power of that magnitude may not be achievable by exciting with a single low frequency due to the limitations of excitation circuitry. However, a pulse enables having such desired high powers in the low frequency range while enabling a wide frequency spectrum to be contained within the magnetic field. The PEC technique can therefore achieve admirable penetration capability. It can also produce reasonable magnitudes for the resultant magnetic field since the power of low frequencies are very high, while high frequencies too exist with low powers. As a result, this technique has significant versatility over the other EC techniques and therefore is used for condition assessment of a wide variety of materials including ones having ferromagnetic properties [1]. Consequentially, the PEC technique can be identified as the most suitable EC technique for the target application of this thesis, *i.e.*, thickness estimation of critical pipe materials which are electrically conductive and ferromagnetic. Commonly used PEC sensor architectures are described in the following section.

2.2 Commonly Used PEC Sensor Architectures

All EC/PEC sensor architectures have in common a solenoid exciter coil for excitation [1]. However, PEC sensor architectures when taken collectively, use separate sensors to detect the magnetic field and therefore differ from the conventional EC sensor architecture which uses the exciter coil alone (Fig. 2.1) to measure the impedance change. PEC sensor architectures can be classified based on the type of detector used. Typically used detectors are solenoid coils, superconducting quantum interference devices (SQUIDs) and Hall-effect and magnetoresistive sensors [1]. With respect to the target application of conductive ferromagnetic material inspection, this chapter classifies PEC sensor architectures into the two categories: (a) Detector coil based architecture; and (b) Non-Detector coil based architecture. The former category simply refers to sensors which use solenoid coils as detectors to sense the magnetic field whereas the latter includes sensors which incorporate the rest of the sensing devices, *i.e.*, SQUIDs, Hall-effect sensors and magnetoresistive sensors.

2.2.1 Detector Coil Based PEC Sensor Architecture

The detector coil based architecture simply uses a solenoid coil to detect the magnetic field via sensing the induced voltage or current across the coil. This is easily the most commonly used architecture for thickness estimation of ferromagnetic materials [2–4, 6, 14, 19, 30, 31]. Desirable thickness discriminative capability possessed by the signals produced by this architecture is the major reason for the common use. This architecture can hence be considered suitable for critical pipe assessment and this thesis deals explicitly with this architecture due to the sensor partnering with this work (Fig. 1.1) is of the typical detector coil based architecture. The cross-sectional view of the configuration of this architecture is shown in Fig. 2.2. A limitation of this architecture is the low resolution since a coil which has a considerable size is used as the detector. Therefore, this architecture has limited sensitivity to fine and isolated defects, but can detect an averaged representation of the material thickness or volume remaining under the footprint of the sensor [34].

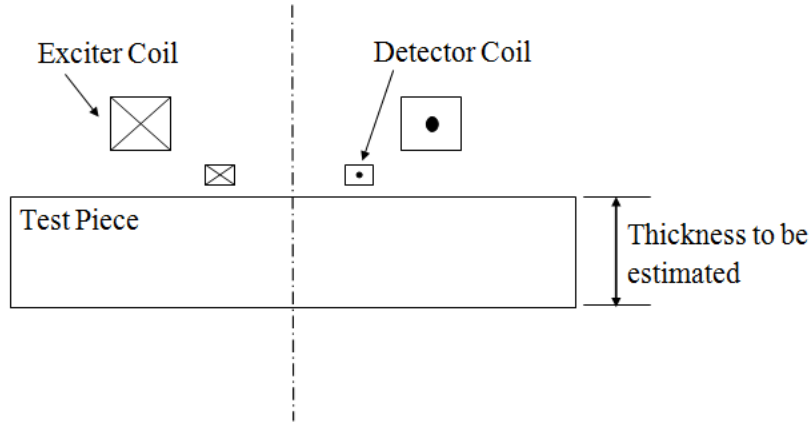


FIGURE 2.2: Cross-sectional view of the typical detector coil based PEC sensor architecture used for ferromagnetic material thickness estimation.

This architecture has coils whose axis is perpendicular to the surface of the test piece. These probes can be either air-core coils or ferrite-core coils. Ferrites have high permeability and the initial coil impedance is higher than that of the air-core coils. Air-cored coils are the ones typically used for ferromagnetic material assessment [2–4, 6, 14, 19, 30, 31, 35]. This architecture is generally suitable for evaluating flat surfaces [1], but this is also used on large diameter pipes [6, 19, 31] as shown in Fig. 1.1 and 2.3 since curvature of large pipes is low relative to the sensor size. Center axis of the cylindrical pipe shown in Fig. 2.3 is perpendicular to the page.

Coils are occasionally arranged in different configurations to obtain variations of this architecture such as Encircling coil probes, Horseshoe-shaped coil probes, Double-function probes, Separate-function probes, Absolute-Mode probes and Differential-Mode probes [1]. These variations are mostly used for nonmagnetic material inspection and RFT sensors used for pipe inspection [20]. Therefore these variations are not of direct relevance to the work of this thesis and are not discussed in detail.

It is known that this architecture is very sensitive to lift-off (vertical distance between an EC/PEC sensor and the surface of the test piece) and tilt [1]. Therefore, it is ideally suited to assess the thickness of flat surfaces by placing the sensor as parallel as possible to the surface. However, when assessing critical pipes, such surface conditions cannot be expected due to the nonmagnetic substances such as rust and graphite being present between the sensor and the ferromagnetic material. As a result, using this architecture for

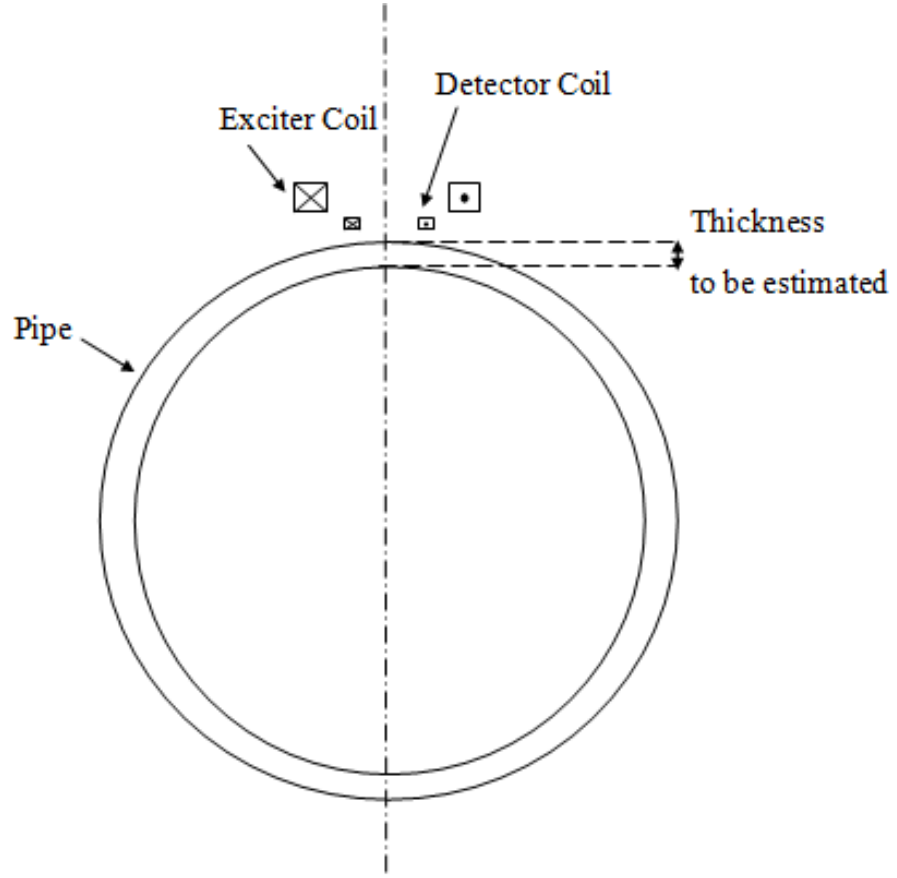


FIGURE 2.3: Cross-sectional view of the typical detector coil based PEC sensor architecture used for pipe thickness assessment (The figure is not drawn to scale).

critical pipe evaluation with the use of existing signal processing and feature extraction techniques is not straightforward. To address the issue, this thesis proposes the “detector coil voltage decay rate” as a signal feature relevant to this architecture since it exhibits desirably reasonable insensitivity to lift-off as shown in the chapters to follow.

2.2.2 Non-Detector Coil Based PEC Sensor Architecture

The non-detector coil based architecture uses magnetic sensors such as SQUIDs, Hall-effect sensors and magnetoresistive sensors to detect the magnetic field instead of the detector coil in the previous architecture [1]. This architecture is not commonly used for ferromagnetic material assessment, however, it has been used on a few occasions with limited applicability [13, 32, 33]. Most commonly this architecture is used for thickness estimation [36], defect detection [37] and achieving lift-off invariance [38, 39] in relation

to nonmagnetic materials. An advantage of this architecture is the use of small magnetic sensors instead of large detector coils enabling it to achieve higher resolution than the detector coil based architecture.

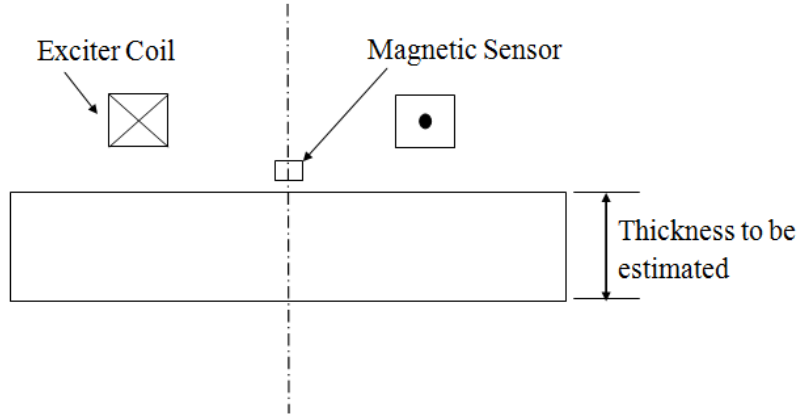


FIGURE 2.4: Cross-sectional view of the typical non-detector coil based PEC sensor architecture.

A magnetoresistive sensor has been used in [13] to assess carbon steel pipe wall thicknesses up to 10 mm. Reference [33] has presented a way of using a Hall-effect sensor supported by a ferrite core to evaluate stainless steel thicknesses up to 5 mm. Using magnetization to improve the sensitivity of a sensor is proposed in [32] to detect and quantify subsurface defects in ferromagnetic steels. It is hence evident that when this architecture is used to assess ferromagnetic materials, it has been mostly applied on low thickness steels. The objective of this thesis however, is not only to assess steels, but also to assess gray and ductile cast irons having thicknesses up to 30 mm. Work which suggest the usability of this architecture on nonlinear and inhomogeneous ferromagnetic materials such as cast irons having high thicknesses is rare and consequentially this architecture is not preferred for the work of this thesis.

2.3 PEC Based Ferromagnetic Material Thickness Quantification

Since the rationale behind selecting the PEC inspection technique and the detector coil based architecture for the target application of this thesis have been clarified, this section

focuses on reviewing previous PEC related work in conductive ferromagnetic material thickness estimation and highlighting application specific signal noise suppression and thickness discriminative feature extraction techniques.

2.3.1 Application Specific Noise Suppression Techniques

PEC signals are time varying induced voltages or currents in the detector due to the net magnetic field resulting from excitation and electromagnetic interaction with the test piece. Signals resulting from excitations used in practice are usually small in magnitude and do not exceed the millivolt scale irrespective of the type of detector. Given the small magnitude of signals, they are highly susceptible to noise [40]. Therefore, appropriate signal conditioning, noise suppression and amplification are essential to acquire signals in the quality suitable for extracting discriminative features to perform condition assessment.

Signal conditioning done in hardware is no different from any standard signal acquisition device as long as minimal distortion is introduced. Amplification and filtering are usually done before sampling and storing the signals. Operational amplifier based amplification [41] and active filtering [42] techniques are used as in any common low voltage electronic system. The thesis [40] has presented the complete design and implementation steps of a PEC system. In [40], a second order Sallen and Key [43] low pass filter is used and amplification is done using an instrumentation amplifier [44] before digital sampling. The hardware signal conditioning methods are not fixed by any means and there is freedom to use any filtering [42] and amplification [41] mechanism depending on the desired signal quality expected at the input of the sampling stage, however, minimal distortion is desired.

Digital sampling networks are known to introduce noises which are unique to the sampling circuitry, and therefore software based signal noise suppression is required to further cleanse the signals [40]. When it comes to software based noise suppression, there are a few unique techniques which are used on PEC signals [40]. Some tailor made methods for signals captured using detector coils have been researched and published as well [2, 3].

As in hardware filtering, the desired feature in software based filtering techniques used on PEC signals is introducing minimal distortion since preserving the original shape of

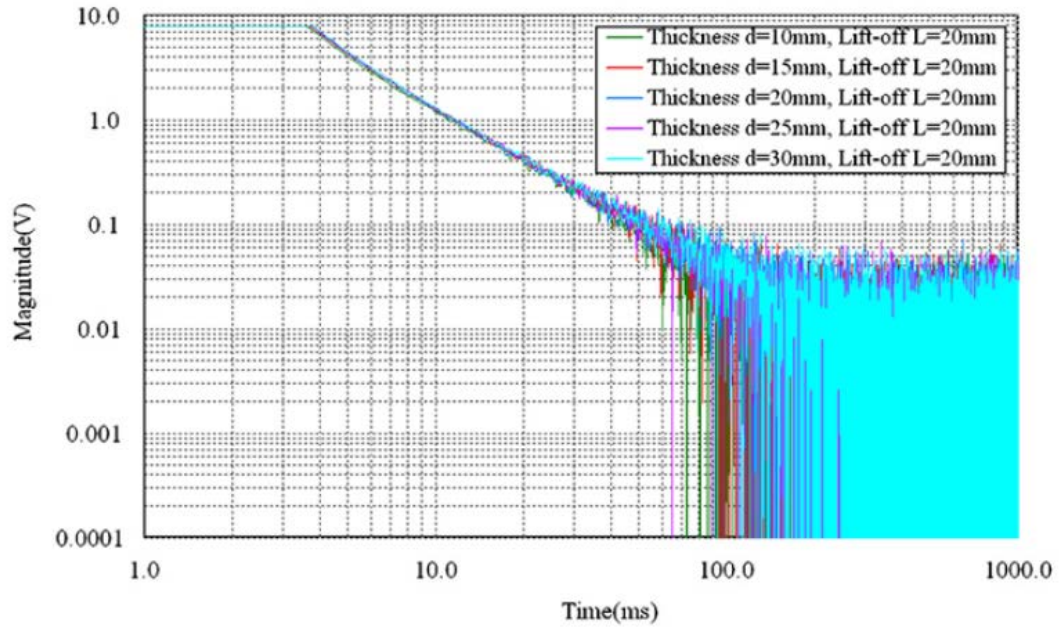
signals is essential to derive relationships between test piece geometry and signal features. Therefore, software implemented counterparts of commonly used filtering techniques such as Chebyshev, Butterworth and Bessel [45, 46], are not generally used due to their tendency to introduce distortion. Instead, techniques such as acquiring multiple signals and averaging, Mean filtering and Gaussian filtering are used [40].

Averaging multiple signals which are synchronized is a useful distortion free noise suppression technique and is used in the digital signal processing stage of the commercial PEC signal acquisition unit (Fig. 1.1) used in this thesis. Mean and Gaussian filters have been examined only on signals acquired by means of magnetic sensors (e.g. Hall-effect) as done in [40] and therefore not used for this work where signals are acquired by means of a detector coil. On the contrary, the techniques proposed in [2] and [3] are applied explicitly on detector coil based signals and are more relevant to this thesis.

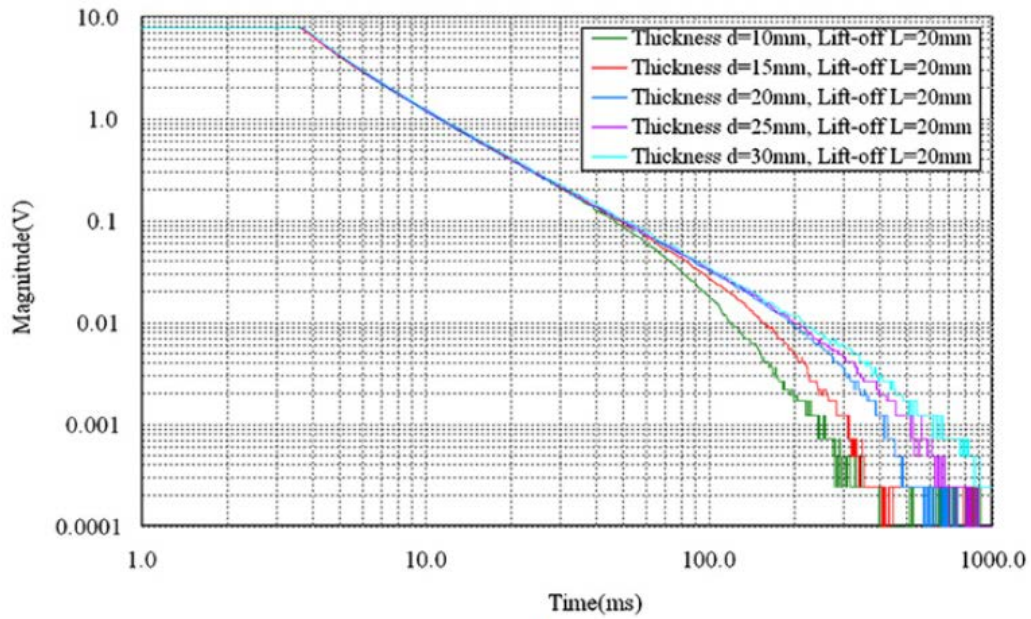
Reference [2] introduces a noise suppression method which improves the signal to noise ratio (SNR) up to about 40 dB. Improvement of signal discriminative capability resulted by filtering can clearly be seen in Fig. 2.5. The signals have been acquired for different thicknesses of steel using a step wedge Q235 steel plate at a constant lift-off of 20 mm. Steps included in the noise suppression method are:

1. Recording multiple PEC signals and calculating the averaged PEC signal.
2. Performing double logarithmic transform of the averaged PEC signal (refers to expressing both signal voltage and time in logarithmic scale).
3. Processing the signal from step(2) by median filtering.
4. Performing an invert signal transformation to Cartesian domain (optional).

As mentioned before, signals of [2] are detector coil based and are very similar to the signals worked with in this thesis, and recording multiple signals and averaging is done in the digital signal processing stage of the PEC signal capturing unit used in this thesis. However, averaging alone is insufficient to obtain desired signal quality. That is why [2] has proposed using a median filter to further suppress the noise. As seen by the results, median filtering can be considered to be very effective in suppressing detector coil based



(a)



(b)

FIGURE 2.5: Detector coil based PEC signals processed in [2], acquired on Q235 steel:
 (a) Signals before filtering; (b) Signals after filtering

PEC signal noise. However, median filters too may introduce distortion if the filter order is not properly selected [47] and therefore is not employed for signal processing in this thesis.

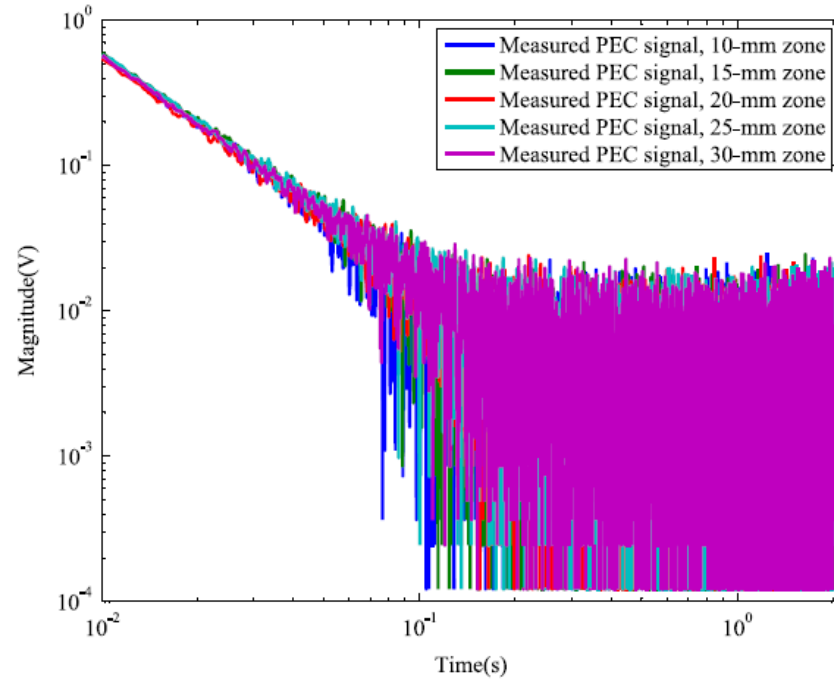
Reference [3] introduces a distortion free noise suppression technique based on numerical cumulative integration. Fig. 2.6 shows signals processed in [3] and the signals have been acquired on different thicknesses of Q235 steel.

The time domain PEC signal (voltage induced in the detector coil) is integrated over time and an analytical model is fitted by approximating the cumulative integration of noise (average over time) to zero. Certain estimated analytical model parameters exhibit functional behavior usable to quantify thickness of ferromagnetic plates. This noise suppression technique is highly desirable for PEC signal processing since it does not introduce distortion and therefore was considered incorporable for the work of this thesis. The approach of approximating average of noise to zero is exploited in this thesis to fit a straight line to the late stage of the induced detector coil voltage to extract the “detector coil voltage decay rate” signal feature. Hence, the procedure followed in this thesis to extract the proposed feature uses the fundamental of approximating average noise to zero as done in [3]. Advantages and disadvantages of the noise suppression techniques in relation to the target application of this thesis are summarized in Table 2.1.

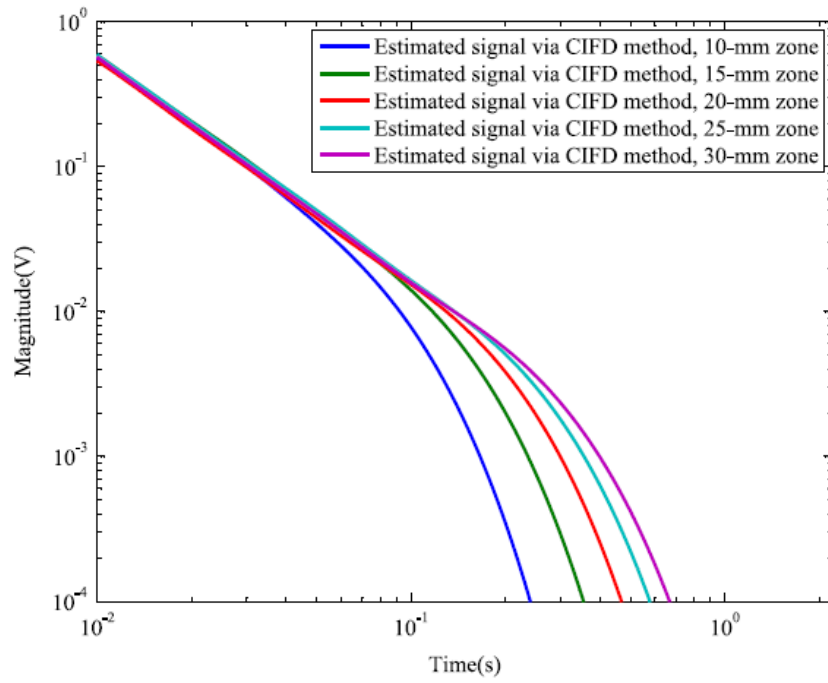
2.3.2 Thickness Discriminative Feature Extraction Techniques

Traditional PEC signal features used for metal test piece property and defect quantification can be classified as: time domain signal features [14, 39], frequency spectrum features [33, 48, 49], principal components [50, 51] and integral features [52]. Among those works related to traditional features, [14] is related to ferromagnetic materials and [33] and [48] are related to evaluating stainless steel thicknesses up to 5 mm. The rest have all been evaluated on non-ferromagnetic materials with non-detector coil based sensors, therefore, they are not directly related to the this thesis.

References [33] and [48] use Hall-effect sensors to evaluate thickness of stainless steel by using features of the power spectral density to discriminate thickness. However, thickness sensitivity has been evaluated only up to 5 mm. Since the signals are acquired using Hall-effect sensors and not detector coils, the feature extraction methods are not directly incorporable with this thesis. Further, the features have not been evaluated on higher thicknesses and other ferromagnetic magnetic materials such as gray and ductile cast



(a)



(b)

FIGURE 2.6: Detector coil based PEC signals processed in [3], acquired on Q235 steel:
 (a) Signals before processing; (b) Signals after processing

TABLE 2.1: Summary of advantages and disadvantages of the application specific signal noise suppression techniques in relation to the target application of this thesis.

Technique	Advantages	Disadvantages	Used in this thesis?
Hardware filtering [40]	Useful as the first stage of filtering.	Requires complex hardware, likely to introduce high distortion if not properly designed.	Yes (Embedded within the commercial kit)
Averaging multiple signals [2, 40]	Digitally implementable, distortion free.	Requires synchronization.	Yes (Embedded within the commercial kit)
Mean filtering [40]	Digitally implementable.	Tested on non-detector coil based signals, may introduce distortion if the window width is not properly selected	No
Gaussian filtering [40]	Digitally implementable.	Tested on non-detector coil based signals, may introduce distortion if the window width is not properly selected	No
Median filtering [2]	Digitally implementable.	May introduce distortion if the filter order is not properly selected	No
Analytical model fitting [3]	Digitally implementable, distortion free.	Minimal, requires determining the analytical model which describes the underlying noise free signal	Yes

irons, which are materials of interest for this thesis. Therefore, the feature extraction methods proposed in [33] and [48] are not incorporated in this thesis.

The detector coil based architecture is used in [14] with the main purpose of finding an efficient and easy-to-use signal feature for the assessment of ferromagnetic pipe wall thinning. Analytical modeling for a detector coil based PEC probe placed over an insulated piping system is performed and its result is verified by experimental test. Two commonly used time-related features, the peak value and the time-to-peak, are found in the differential signal obtained by subtracting the test signal from a reference signal. The time-to-peak is found to be superior to the peak value due to its linear variation with wall thickness.

Influences of various conditions in practical testing on the PEC signal are investigated. Results show that the time-to-peak is independent of the insulation thickness and the probe lift-off. Robustness of time-to-peak to probe configuration is also validated by employing three probes of different dimensions and structures. To determine the linear range of time-to-peak with amount of wall thinning, differential signals based on different reference thicknesses are examined. However, results show that the time-to-peak only keeps linear for relative wall thinning less than 60%, which is a drawback and therefore this feature extraction technique is not used in this thesis. Despite that the technique could still be useful for calibration purposes in periodical in-service inspection of insulated pipelines.

Publications [20] and [32] focus on defect identification in ferromagnetic materials. In [20], a remote field eddy current sensor (RFT) has been energized by a PEC excitation to detect axisymmetric surface slot defects on ferromagnetic tubes by examining the variations of the induced detector coil voltage features. However, since the RFT sensing technique is used and the fact that the focus is on defect detection, this work cannot be coupled with this thesis. Using magnetization to improve the sensitivity of the time domain reference subtracted PEC difference signal features was proposed in [32] to detect and quantify subsurface defects in ferromagnetic steels. Although the features used in [20] and [32] are effective on defects, their effectiveness on ferromagnetic material thickness quantification has not been examined, as a result those feature extraction techniques are not incorporated in this thesis.

Several analytical methods which are directly related to ferromagnetic material thickness quantification have been proposed [4, 36, 53]. Such methods are the most closely related ones to the focus of this thesis. References [36] and [53] follow similar approaches in modeling Hall-effect sensor readings and PEC difference signals respectively, when used on non-ferromagnetic materials. In the context of ferromagnetic materials however, sensitivity of those sensing techniques to thickness have not been evaluated and consequently, those techniques are not made use of in this thesis.

Recent work [3] and [4] have proposed methods of fitting analytical models for detector coil based PEC sensor signals. Those publications exhibit the appreciable thickness sensitivity of the induced detector coil voltage to ferromagnetic material thickness. Thickness

sensitivity up to 25 to 30 mm have been achieved for steel. Having sensitivity up to about 30 mm is greatly desired for critical pipe evaluation. The gray cast iron pipes which are evaluated in this thesis have maximum thicknesses up to 30 mm [9]. Therefore, the analytical model for PEC detector coil voltage used in [3] and [4] is exploited in this thesis. The “detector coil voltage decay rate” signal feature proposed in this thesis is derived starting from that analytical model.

In [4] where the analytical model was first published, a detector coil based PEC sensor placed above a conductive ferromagnetic plate is modeled as an infinite set of mutually coupled coils. That analysis yields an analytical model in the form of an infinite summation of exponentials, to the induced detector coil voltage (PEC signal). This analytical model is then fitted to experimentally captured PEC signals by estimating model parameters [3, 4]. Some model parameters exhibit monotonic variation with thickness up to about 30 mm. It is suggested that such model parameters may be used for in situ ferromagnetic material condition assessment purposes such as critical pipe assessment. However, [3] and [4] have not developed and validated complete frameworks on in situ pipes. Therefore, the objective of this thesis has not been accomplished in those works. This thesis hence builds upon the theoretical models used in [3] and [4] to propose a novel PEC signal feature which shows some low dependence to lift-off, sensor shape, and size; and use the feature to learn a thickness-feature function, and use the learned function to estimate wall thickness of in situ critical water pipes.

A similar analytical model for the detector coil based PEC architecture has been proposed in [54] and it has been used to simultaneously quantify material properties and thickness of carbon steel by fitting to PEC data and estimating model parameters [35]. However, that model is defined for concentric circular sensors, hence cannot be used with non-circular sensors; and that approach requires the lift-off to be accurately known. In critical pipe related applications, pipe surfaces are not always clean and the healthy ferromagnetic material is often covered by corrosion and graphitization layers. Therefore, knowing an accurate measure of lift-off is not always possible. Therefore, although the model parameter estimation methods do perform well in thickness assessment of flat plates at constant and supposedly known lift-offs, they do comprise vulnerabilities in relation to the particular application of in situ critical pipe evaluation. That is why the “detector coil voltage decay rate” feature

introduced in this thesis is required since it demonstrates low dependence on lift-off, and some other factors which makes the feature immune to practical challenges encountered during in situ critical pipe wall thickness assessment. Consequentially, this thesis brings novelty by introducing a PEC signal feature having a significant lift-off invariance which is suitable for in situ critical pipe assessment. Aspects associated with previously proposed feature extraction techniques which limit their applicability for the work of this thesis are summarized in Table 2.2.

TABLE 2.2: Aspects associated with previously proposed feature extraction techniques which limit their applicability for the work of this thesis.

References	Technique	Limiting Aspects
[33, 48]	Power spectral density features.	Analysis done only on stainless steel, thickness sensitivity reported up to 5 mm, study based on Hall-effect sensors.
[14]	Features of the time domain difference signal.	Limited applicability, linearity observed for relative wall thinning less than 60%.
[20, 32]	Features of the detector coil voltage.	Focused on defect identification, possibility of thickness discrimination not reported.
[36, 53]	Analytical modeling of Hall device readings and difference signals.	Tested only on non-ferromagnetic materials
[3, 4, 35, 54]	Analytical model parameter estimation.	Lift-off insensitivity not demonstrated, have not been evaluated on in situ ferromagnetic pipes.

2.4 Effect of PEC Sensor Geometry on Measurement Capabilities

Resolution of the detector coil based PEC sensor architecture is limited by the size of the detector coil, and in general, the size of the sensor. In simple terms, larger the sensor, larger the region impacted by the magnetic field will be, and consequently, the interpreted condition will be an averaged representation of a large region of the test piece [34]. Though the resolution can be increased by reducing the size, that limits the spread

of the magnetic field and results in not being able to assess thick material since the eddy current penetration depth will be lower. Theoretically, it can be argued that increasing the strength of excitation will compromise the reduction of magnetic field spread caused by the reduction of size. But then again, the amount of increase allowable to the excitation is limited by the available electronic circuitry and related hardware. Therefore, for a given strength of excitation, achieving deep penetration can usually be done at the cost of sacrificing resolution [40].

Studies on the effect of PEC sensor geometry on measurement capabilities are rare. The doctoral thesis [40] presents a fairly comprehensive FEA based numerical study on the influence of shielding, including and excluding a ferrite core and the size of the excitation coil on eddy current penetration and lateral spread caused by a Hall-effect based PEC sensor. There is no exact analytical technique to determine the most effective design and sensor size [40]. The study has found that shielding has a tendency to increase penetration depth while reducing the lateral spread, which are desirable characteristics. Including a core has the tendency to further reduce the lateral spread which is desirable again, but that will also reduce the penetration depth which is undesired. In addition, the influence of the geometry of the excitation coil has also been studied. The findings are:

1. The larger the internal radius, the deeper the penetration and the larger the lateral spread of eddy currents.
2. The larger the outer radius, the deeper the penetration and the larger the lateral spread of eddy currents.
3. The smaller the height, the deeper the penetration and the larger the lateral spread of eddy currents.

Though [40] has presented important knowledge on the effect of the excitation coil geometry on the spread of eddy currents, the study is limited to non-ferromagnetic materials. Further, the effect of sensor geometry on the sensitivity of thickness discriminative signal features based on the detector coil architecture has not been studied.

Since a study on ferromagnetic materials has not been done in [40], this thesis brings forth a detailed numerical study (using FEA) to aid understanding the influence of detector

coil based sensor geometry on the thickness discriminative capability of the “detector coil voltage decay rate” signal feature. The objective is to find how the sensor resolution can be increased so that the detection of fine and isolated flaws on ferromagnetic materials becomes viable.

2.5 Conclusions

This chapter reviewed the various EC inspection techniques and clarified the necessity of the PEC technique for geometric condition assessment of conductive ferromagnetic materials. Various PEC sensor architectures were then reviewed and the use of the detector coil based architecture for the target application of this thesis was justified. Application specific signal conditioning and noise suppression techniques were reviewed while discussing the importance of distortion free signal processing. The distortion free noise suppression methods of fitting analytical models to noisy signals by approximating the average noise to be zero was identified as the method suitable for the target application of this thesis. Existing ferromagnetic material thickness discriminative feature extraction techniques were reviewed eventually. The fact that the influence of lift-off on proposed features not being studied and quantified was identified as a limitation in the usability of the available feature extraction techniques in complex scenarios like critical pipe evaluation. Therefore, the requirement of the novel signal feature introduced in this thesis is warranted. Finally, existing knowledge on the influence of sensor geometry on measurement capabilities was reviewed. Previous studies were found to be limited to effects on eddy current penetration depth and lateral flow in non-ferromagnetic materials. Therefore, room for analyzing the impact on the sensitivity of thickness discriminative signal features for ferromagnetic materials and the effect of sensor geometry on measurement was identified.

Bibliography

- [1] J. García-Martín, J. Gómez-Gil, and E. Vázquez-Sánchez, “Non-destructive techniques based on eddy current testing,” *Sensors*, vol. 11, no. 3, pp. 2525–2565, 2011.
- [2] C. Huang, W. Xinjun, X. Zhiyuan, and Y. Kang, “Pulsed eddy current signal processing method for signal denoising in ferromagnetic plate testing,” *NDT & E International*, vol. 43, no. 7, pp. 648–653, 2010.
- [3] C. Huang and X. Wu, “An improved ferromagnetic material pulsed eddy current testing signal processing method based on numerical cumulative integration,” *NDT & E International*, vol. 69, pp. 35–39, 2015.
- [4] C. Huang, X. Wu, Z. Xu, and Y. Kang, “Ferromagnetic material pulsed eddy current testing signal modeling by equivalent multiple-coil-coupling approach,” *NDT & E International*, vol. 44, no. 2, pp. 163–168, 2011.
- [5] J. Rudd and M. Roubal, “Broadband electro-magnetic technique for advanced condition assessment and pipe failure prediction of water infrastructure,” in *Ozwater Conference, 2014*. <http://www.awa.asn.au/html/emails/Ozwater14/pdf/natozw14Final00366.pdf>, last access date: 11/01/2015.
- [6] N. Ulapane, A. Alempijevic, T. Vidal-Calleja, J. V. Miro, J. Rudd, and M. Roubal, “Gaussian process for interpreting pulsed eddy current signals for ferromagnetic pipe profiling,” in *Industrial Electronics and Applications (ICIEA), 2014 IEEE 9th Conference on*, pp. 1762–1767, IEEE, 2014.

-
- [7] K. L. Rens, T. J. Wipf, and F. W. Klaiber, "Review of nondestructive evaluation techniques of civil infrastructure," *Journal of performance of constructed facilities*, vol. 11, no. 4, pp. 152–160, 1997.
- [8] R. B. Petersen and R. E. Melchers, "Long-term corrosion of cast iron cement lined pipes," *Corrosion and Prevention*, pp. 11–14, 2012.
- [9] J. V. Miro, J. Rajalingam, T. Vidal-Calleja, F. de Bruijn, R. Wood, D. Vitanage, N. Ulapane, B. Wijerathna, and D. Su, "A live test-bed for the advancement of condition assessment and failure prediction research on critical pipes," *Water Asset Management International*, ISSN Print: 1814-5434, ISSN Online: 1814-5442, vol. 10, no. 2, pp. 03–08, 2014.
- [10] D. Vitanage, J. Kodikara, and G. Allen, "Collaborative research on condition assessment and pipe failure prediction for critical water mains," *Water Asset Management International*, vol. 10, pp. 15–18, 2014.
- [11] R. Petersen, M. Dafter, and R. Melchers, "Long-term corrosion of buried cast iron water mains: field data collection and model calibration," *Water Asset Management International*, vol. 9, pp. 13–17, 2013.
- [12] Z. Liu and Y. Kleiner, "State of the art review of inspection technologies for condition assessment of water pipes," *Measurement*, vol. 46, no. 1, pp. 1–15, 2013.
- [13] W. Cheng, "Pulsed eddy current testing of carbon steel pipes wall-thinning through insulation and cladding," *Journal of Nondestructive Evaluation*, vol. 31, no. 3, pp. 215–224, 2012.
- [14] Z. Xu, X. Wu, J. Li, and Y. Kang, "Assessment of wall thinning in insulated ferromagnetic pipes using the time-to-peak of differential pulsed eddy-current testing signals," *NDT & E International*, vol. 51, pp. 24–29, 2012.
- [15] J. R. Davis, "ASM specialty handbook: cast irons," *ASM International*, vol. 124, pp. 433–435, 1996.
- [16] J.-M. Jin, *The finite element method in electromagnetics*. John Wiley & Sons, 2014.
- [17] B. A. Szabo and I. Babuška, *Finite element analysis*. John Wiley & Sons, 1991.

-
- [18] C. E. Rasmussen and C. K. I. Williams, “Gaussian processes for machine learning,” *The MIT Press, 2006, ISBN: 0-262-18253-X*, 2006.
- [19] N. Ulapane, A. Alempijevic, and V.-C. T. Miro, Jaime Valls, “Nondestructive evaluation of ferromagnetic material thickness using pulsed eddy current sensor detector coil voltage decay rate,” *NDT & E International*, 2015. Under Review.
- [20] D. Vasic, V. Bilas, and D. Ambrus, “Pulsed eddy-current nondestructive testing of ferromagnetic tubes,” *Instrumentation and Measurement, IEEE Transactions on*, vol. 53, no. 4, pp. 1289–1294, 2004.
- [21] H. Hashizume, Y. Yamada, K. Miya, S. Toda, K. Morimoto, Y. Araki, K. Satake, and N. Shimizu, “Numerical and experimental analysis of eddy current testing for a tube with cracks,” *Magnetics, IEEE Transactions on*, vol. 28, no. 2, pp. 1469–1472, 1992.
- [22] C. V. Dodd and W. E. Deeds, “Analytical solutions to eddy-current probe-coil problems,” *Journal of applied physics*, vol. 39, no. 6, pp. 2829–2838, 1968.
- [23] S. Sharma, “Application of finite element models to eddy current probe design for aircraft inspection,” 1998. Doctoral Thesis, Digital Repository, Iowa State University, <http://lib.dr.iastate.edu/>.
- [24] F. Thollon, B. Lebrun, N. Burais, and Y. Jayet, “Numerical and experimental study of eddy current probes in ndt of structures with deep flaws,” *NDT & E International*, vol. 28, no. 2, pp. 97–102, 1995.
- [25] J. R. Bowler, Y. Yoshida, and N. Harfield, “Vector-potential boundary-integral evaluation of eddy-current interaction with a crack,” *Magnetics, IEEE Transactions on*, vol. 33, no. 5, pp. 4287–4294, 1997.
- [26] J. H. Rose, E. Uzal, and J. C. Moulder, “Magnetic permeability and eddy-current measurements,” in *Review of progress in quantitative nondestructive evaluation*, pp. 315–322, Springer, 1995.

- [27] A. Pirani, M. Ricci, R. Specogna, A. Tamburrino, and F. Trevisan, “Multi-frequency identification of defects in conducting media,” *Inverse Problems*, vol. 24, no. 3, p. 035011, 2008.
- [28] W. Yin and A. J. Peyton, “Thickness measurement of non-magnetic plates using multi-frequency eddy current sensors,” *NDT & E International*, vol. 40, no. 1, pp. 43–48, 2007.
- [29] Y. Le Diraison, P.-Y. Joubert, and D. Placko, “Characterization of subsurface defects in aeronautical riveted lap-joints using multi-frequency eddy current imaging,” *NDT & E International*, vol. 42, no. 2, pp. 133–140, 2009.
- [30] X. Chen and Y. Lei, “Excitation current waveform for eddy current testing on the thickness of ferromagnetic plates,” *NDT & E International*, vol. 66, pp. 28–33, 2014.
- [31] X. Chen and Y. Lei, “Time-domain analytical solutions to pulsed eddy current field excited by a probe coil outside a conducting ferromagnetic pipe,” *NDT & E International*, 2014, 2014.
- [32] A. Sophian, G. Y. Tian, D. Taylor, and J. Rudlin, “Flaw detection and quantification for ferromagnetic steels using pulsed eddy current techniques and magnetization,” *Transactions on Engineering Sciences*, vol. 44, pp. 381–390, 2003.
- [33] D. G. Park, C. S. Angani, G. D. Kim, C. G. Kim, and Y. M. Cheong, “Evaluation of pulsed eddy current response and detection of the thickness variation in the stainless steel,” *Magnetics, IEEE Transactions on*, vol. 45, no. 10, pp. 3893–3896, 2009.
- [34] C. Waters, “Rdt-incotest® for the detection of corrosion under insulation,” *NON DESTRUCTIVE TESTING AUSTRALIA*, vol. 36, no. 5, pp. 124–129, 1999.
- [35] V. O. De Haan and P. J. de Jong, “Simultaneous measurement of material properties and thickness of carbon steel plates using pulsed eddy currents,” in *16th World Conference on Non-Destructive Testing in Montreal*, 2004.
- [36] Y. Li, G. Y. Tian, and A. Simm, “Fast analytical modelling for pulsed eddy current evaluation,” *NDT & E International*, vol. 41, no. 6, pp. 477–483, 2008.

-
- [37] A. Sophian, G. Y. Tian, D. Taylor, and J. Rudlin, "Design of a pulsed eddy current sensor for detection of defects in aircraft lap-joints," *Sensors and Actuators A: Physical*, vol. 101, no. 1, pp. 92–98, 2002.
- [38] G. Y. Tian and A. Sophian, "Reduction of lift-off effects for pulsed eddy current ndt," *NDT & E International*, vol. 38, no. 4, pp. 319–324, 2005.
- [39] G. Y. Tian, Y. Li, and C. Mandache, "Study of lift-off invariance for pulsed eddy-current signals," *Magnetics, IEEE Transactions on*, vol. 45, no. 1, pp. 184–191, 2009.
- [40] A. Sophian, "Characterisation of surface and sub-surface discontinuities in metals using pulsed eddy current sensors," 2003. Doctoral thesis, University of Huddersfield, <http://eprints.hud.ac.uk/6916/>.
- [41] J. Huijsing, *Operational amplifiers: theory and design*. Springer Science & Business Media, 2011.
- [42] T. Kugesstadt, "Active filter design techniques. texas instruments."
- [43] S. Niewiadomski, *Filter handbook: a practical design guide*. Newnes, 1989.
- [44] C. Kitchin and L. Counts, *A designer's guide to instrumentation amplifiers*. Analog Devices, 2006.
- [45] T. Deliyannis, Y. Sun, and J. K. Fidler, *Continuous-time active filter design*. Crc Press, 2010.
- [46] M. D. Lutovac, D. V. Tošić, and B. L. Evans, *Filter design for signal processing using MATLAB and Mathematica*. Miroslav Lutovac, 2001.
- [47] F. Xuan, L. Cai, Y. Baojun, L. Zhe, Z. Fengqin, and L. Yang, "The impacts of median filter to the phases and shapes of signals," *GEOPHYSICAL PROSPECTING FOR PETROLEUM*, vol. 41, no. 1, pp. 37–41, 2002.
- [48] C. S. Angani, D. G. Park, G. D. Kim, C. G. Kim, and Y. M. Cheong, "Differential pulsed eddy current sensor for the detection of wall thinning in an insulated stainless steel pipe," *Journal of Applied Physics*, vol. 107, no. 9, p. 09E720, 2010.

- [49] Y. He, M. Pan, F. Luo, and G. Y. Tian, “Pulsed eddy current imaging and frequency spectrum analysis for hidden defect nondestructive testing and evaluation,” *NDT & E International*, vol. 44, no. 4, pp. 344–352, 2011.
- [50] A. Sophian, G. Y. Tian, D. Taylor, and J. Rudlin, “A feature extraction technique based on principal component analysis for pulsed eddy current ndt,” *NDT & E International*, vol. 36, no. 1, pp. 37–41, 2003.
- [51] G. Y. Tian, A. Sophian, D. Taylor, and J. Rudlin, “Multiple sensors on pulsed eddy-current detection for 3-d subsurface crack assessment,” *IEEE Sensors Journal*, vol. 5, no. 1, pp. 90–96, 2005.
- [52] D. Chen, Q. Ji, H. Zhang, and L. Zhao, “Application of pulsed eddy current in plate thickness evaluation,” in *Proceedings of the 4th IEEE Conference on Industrial Electronics and Applications, IEEE ICIEA*, pp. 3286–3288, IEEE, 2009.
- [53] M. Fan, P. Huang, B. Ye, D. Hou, G. Zhang, and Z. Zhou, “Analytical modeling for transient probe response in pulsed eddy current testing,” *NDT & E International*, vol. 42, no. 5, pp. 376–383, 2009.
- [54] V. O. De Haan and P. A. De Jong, “Analytical expressions for transient induction voltage in a receiving coil due to a coaxial transmitting coil over a conducting plate,” *IEEE Transactions on Magnetics*, vol. 40, no. 2, pp. 371–378, 2004.
- [55] S. Boyd and L. Vandenberghe, *Convex optimization*. Cambridge university press, 2004.
- [56] A. W. Roberts and D. E. Varberg, *Convex functions*. Elsevier, 1973.
- [57] R. R. Phelps, *Convex functions, monotone operators and differentiability*. Springer-Vlg, 1989.
- [58] “Engineering information - cast iron pipe data.” A data sheet from Mueller Co., REV 4-99.
- [59] “Materials specification 1 for ductile iron pipe.” Denver Water, Engineering Standards 14th Edition, March 2012.

-
- [60] “Atlas tech note no. 12, pipe dimensions.” Atlas Steels, January 2011.
- [61] G. Golub, “Numerical methods for solving linear least squares problems,” *Numerische Mathematik*, vol. 7, no. 3, pp. 206–216, 1965.
- [62] C. Multiphysics, “Comsol multiphysics user guide (version 4.3 a),” *COMSOL, AB*, 2012.
- [63] “Physical property measurement system.” AC Measurement System (ACMS) Option Users Manual, Quantum Design, Part Number 1084-100 C-1.
- [64] “Ppms, physical property measurement system.” Quantum Design, 1070-002, Rev. A0.
- [65] B. Skinner, J. Vidal-Calleja, Teresa amd Valls Miro, F. De Bruijn, and R. Falque, “3D point cloud upsampling for accurate reconstruction of dense 2.5D thickness maps,” in *Proceedings of the Australasian Conference on Robotics and Automation 2014 (ACRA 2014)*, (Melbourne, Australia), pp. 1–7, Australian Robotics and Automation Association Inc., 2014.
- [66] T. Vidal-Calleja, D. Su, F. De Bruijn, and J. V. Miro, “Learning spatial correlations for bayesian fusion in pipe thickness mapping,” in *Robotics and Automation (ICRA), 2014 IEEE International Conference on*, pp. 683–690, IEEE, 2014.
- [67] J. R. Bowler, “Eddy-current interaction with an ideal crack. i. the forward problem,” *Journal of Applied Physics*, vol. 75, no. 12, pp. 8128–8137, 1994.
- [68] A. L. Ribeiro, H. G. Ramos, and O. Postolache, “A simple forward direct problem solver for eddy current non-destructive inspection of aluminum plates using uniform field probes,” *Measurement*, vol. 45, no. 2, pp. 213–217, 2012.
- [69] Z. Chen and K. Miya, “Ect inversion using a knowledge-based forward solver,” *Journal of nondestructive evaluation*, vol. 17, no. 3, pp. 167–175, 1998.
- [70] S. J. Norton and J. R. Bowler, “Theory of eddy current inversion,” *Journal of applied physics*, vol. 73, no. 2, pp. 501–512, 1993.

-
- [71] J. R. Bowler, S. J. Norton, and D. J. Harrison, "Eddy-current interaction with an ideal crack. ii. the inverse problem," *Journal of applied physics*, vol. 75, no. 12, pp. 8138–8144, 1994.
- [72] M. Soleimani, W. R. B. Lionheart, A. J. Peyton, X. Ma, and S. R. Higson, "A three-dimensional inverse finite-element method applied to experimental eddy-current imaging data," *Magnetics, IEEE Transactions on*, vol. 42, no. 5, pp. 1560–1567, 2006.
- [73] Y. S. Tarng, S. C. Ma, and L. K. Chung, "Determination of optimal cutting parameters in wire electrical discharge machining," *International Journal of Machine Tools and Manufacture*, vol. 35, no. 12, pp. 1693–1701, 1995.
- [74] D. F. Dauw, H. Sthioul, R. Delpretti, and C. Tricarico, "Wire analysis and control for precision edm cutting," *CIRP Annals-Manufacturing Technology*, vol. 38, no. 1, pp. 191–194, 1989.
- [75] J. C. Lashley, M. F. Hundley, A. Migliori, J. L. Sarrao, P. G. Pagliuso, T. W. Darling, M. Jaime, J. C. Cooley, W. L. Hults, L. Morales, *et al.*, "Critical examination of heat capacity measurements made on a quantum design physical property measurement system," *Cryogenics*, vol. 43, no. 6, pp. 369–378, 2003.
- [76] Q. Shi, C. L. Snow, J. Boerio-Goates, and B. F. Woodfield, "Accurate heat capacity measurements on powdered samples using a quantum design physical property measurement system," *The Journal of Chemical Thermodynamics*, vol. 42, no. 9, pp. 1107–1115, 2010.
- [77] J. Olivier, B. Servet, M. Vergnolle, M. Mosca, and G. Garry, "Stability/instability of conductivity and work function changes of its thin films, uv-irradiated in air or vacuum: Measurements by the four-probe method and by kelvin force microscopy," *Synthetic Metals*, vol. 122, no. 1, pp. 87–89, 2001.
- [78] T. Kanagawa, R. Hobara, I. Matsuda, T. Tanikawa, A. Natori, and S. Hasegawa, "Anisotropy in conductance of a quasi-one-dimensional metallic surface state measured by a square micro-four-point probe method," *Physical review letters*, vol. 91, no. 3, p. 036805, 2003.

-
- [79] V. Desnica, K. Škarić, D. Jembrih-Simbuerger, S. Fazinić, M. Jakšić, D. Mudronja, M. Pavličić, I. Peranić, and M. Schreiner, “Portable xrf as a valuable device for preliminary in situ pigment investigation of wooden inventory in the trski vrh church in croatia,” *Applied Physics A*, vol. 92, no. 1, pp. 19–23, 2008.
- [80] E. Frahm, “An evaluation of portable x-ray fluorescence for artifact sourcing in the field: can a handheld device differentiate anatolian obsidian sources,” in *119th Annual Meeting of The Geological Society of America, Denver*, 2007.
- [81] L. Solymar, D. Walsh, and R. R. A. Syms, *Electrical properties of materials*. Oxford University Press, 2014.
- [82] G. Marom, S. Fischer, F. R. Tuler, and H. D. Wagner, “Hybrid effects in composites: conditions for positive or negative effects versus rule-of-mixtures behaviour,” *Journal of Materials Science*, vol. 13, no. 7, pp. 1419–1426, 1978.
- [83] H. S. Kim, “On the rule of mixtures for the hardness of particle reinforced composites,” *Materials Science and Engineering: A*, vol. 289, no. 1, pp. 30–33, 2000.
- [84] R. W. Pryor, *Multiphysics Modeling Using COMSOL: A First Principles Approach*. Jones & Bartlett Publishers, 2011.
- [85] T. Morisue, “Magnetic vector potential and electric scalar potential in three-dimensional eddy current problem,” *Magnetics, IEEE Transactions on*, vol. 18, no. 2, pp. 531–535, 1982.
- [86] O. Biro and K. Preis, “On the use of the magnetic vector potential in the finite-element analysis of three-dimensional eddy currents,” *Magnetics, IEEE Transactions on*, vol. 25, no. 4, pp. 3145–3159, 1989.
- [87] P. Dular, J. Gyselinck, C. Geuzaine, N. Sadowski, and J. P. A. Bastos, “A 3-d magnetic vector potential formulation taking eddy currents in lamination stacks into account,” *Magnetics, IEEE Transactions on*, vol. 39, no. 3, pp. 1424–1427, 2003.
- [88] R. C. Degeneff, M. R. Gutierrez, S. J. Salon, D. W. Burow, and R. J. Nevins, “Kron’s reduction method applied to the time stepping finite element analysis of induction

- machines,” *Energy Conversion, IEEE Transactions on*, vol. 10, no. 4, pp. 669–674, 1995.
- [89] R.-f. Liu, D.-J. Yan, and M.-q. Hu, “Field circuit and movement coupled time stepping finite element analysis on permanent magnet brushless dc motors,” in *Zhongguo Dianji Gongcheng Xuebao(Proceedings of the Chinese Society of Electrical Engineering)*, vol. 27, pp. 59–64, 2007.
- [90] N. Ida, *Numerical modeling for electromagnetic non-destructive evaluation*, vol. 1. Springer Science & Business Media, 1995.
- [91] P. Monk, *Finite element methods for Maxwell’s equations*. Oxford University Press, 2003.
- [92] A. Taflove and S. C. Hagness, *Computational electrodynamics*. Artech house, 2005.
- [93] D. J. Griffiths and R. College, *Introduction to electrodynamics*, vol. 3. prentice Hall Upper Saddle River, NJ, 1999.
- [94] C. A. Sawicki, “A dynamic demonstration of lenz’s law,” *The Physics Teacher*, vol. 35, no. 1, pp. 47–49, 1997.
- [95] M. K. Roy, M. K. Harbola, and H. C. Verma, “Demonstration of lenz’s law: Analysis of a magnet falling through a conducting tube,” *American Journal of Physics*, vol. 75, no. 8, pp. 728–730, 2007.
- [96] J. B. Bronzan, “The magnetic scalar potential,” *American Journal of Physics*, vol. 39, pp. 1357–1359, 1971.
- [97] R. D. Pillsbury Jr, “A three dimensional eddy current formulation using two potentials: The magnetic vector potential and total magnetic scalar potential,” *Magnetics, IEEE Transactions on*, vol. 19, no. 6, pp. 2284–2287, 1983.
- [98] O. Bíró, K. Preis, G. Buchgraber, and I. Tícar, “Voltage-driven coils in finite-element formulations using a current vector and a magnetic scalar potential,” *IEEE transactions on magnetics*, vol. 40, no. 2, pp. 1286–1289, 2004.
- [99] J. E. Marsden and A. Tromba, *Vector calculus*. Macmillan, 2003.

-
- [100] H. Lass, *Vector and tensor analysis*. 1950.
- [101] H. M. Schey, "Div, grad, curl, and all that: an informal text on vector calculus," *AMC*, vol. 10, p. 12, 1997.
- [102] K.-J. Bathe and E. L. Wilson, "Numerical methods in finite element analysis," 1976.
- [103] C. W. Steele, *Numerical computation of electric and magnetic fields*. Springer Science & Business Media, 2012.
- [104] M. V. K. Chari, "Finite-element solution of the eddy-current problem in magnetic structures," *Power Apparatus and Systems, IEEE Transactions on*, no. 1, pp. 62–72, 1974.
- [105] I. Z. Abidin, G. Y. Tian, J. Wilson, S. Yang, and D. Almond, "Quantitative evaluation of angular defects by pulsed eddy current thermography," *NDT & E International*, vol. 43, no. 7, pp. 537–546, 2010.
- [106] S. Moaveni, *Finite element analysis: theory and application with ANSYS*. Pearson Education India, 2003.
- [107] P. C. Rem, P. A. Leest, and A. J. Van den Akker, "A model for eddy current separation," *International journal of mineral processing*, vol. 49, no. 3, pp. 193–200, 1997.
- [108] H. W. Liu, S. P. Zhan, Y. H. Du, and P. Zhang, "Study on pulsed eddy current non-destructive testing technology for pipeline corrosion defects based on finite element method," in *Applied Mechanics and Materials*, vol. 120, pp. 36–41, Trans Tech Publ, 2012.
- [109] C. Gilles-Pascaud, G. Pichenot, D. Premel, C. Reboud, and A. Skarlatos, "Modelling of eddy current inspections with civa," in *proceedings of the 17th World Conference on Nondestructive Testing, Shanghai, edited on CD-ROM*, vol. 11, 2008.
- [110] C. Reboud, G. Pichenot, D. Premel, and R. Raillon, "2008 ect benchmark results: Modeling with civa of 3d flaws responses in planar and cylindrical work pieces," *Proceedings of the 35th Annual Review of Progress in Quantitative Nondestructive Evaluation*, pp. 1915–1921, 2008.

- [111] F. Vacher, F. Alves, and C. Gilles-Pascaud, “Eddy current nondestructive testing with giant magneto-impedance sensor,” *NDT & E International*, vol. 40, no. 6, pp. 439–442, 2007.
- [112] D. C. Giancoli, *Physics for scientists and engineers with modern physics*. Pearson Education, 2008.
- [113] W. Steinhögl, G. Schindler, G. Steinlesberger, M. Traving, and M. Engelhardt, “Comprehensive study of the resistivity of copper wires with lateral dimensions of 100 nm and smaller,” *Journal of Applied Physics*, vol. 97, no. 2, p. 023706, 2005.
- [114] R. J. Allemang and D. L. Brown, “A correlation coefficient for modal vector analysis,” in *Proceedings of the 1st international modal analysis conference*, vol. 1, pp. 110–116, SEM, Orlando, 1982.
- [115] J. Lee Rodgers and W. A. Nicewander, “Thirteen ways to look at the correlation coefficient,” *The American Statistician*, vol. 42, no. 1, pp. 59–66, 1988.
- [116] R. Taylor, “Interpretation of the correlation coefficient: a basic review,” *Journal of diagnostic medical sonography*, vol. 6, no. 1, pp. 35–39, 1990.
- [117] C. E. Rasmussen, “Gaussian processes in machine learning,” in *Advanced lectures on machine learning*, pp. 63–71, Springer, 2004.
- [118] M. Seeger, “Gaussian processes for machine learning,” *International Journal of Neural Systems*, vol. 14, no. 02, pp. 69–106, 2004.
- [119] N. N. B. Ulapane and S. G. Abeyratne, “Gaussian process for learning solar panel maximum power point characteristics as functions of environmental conditions,” in *Industrial Electronics and Applications (ICIEA), 2014 IEEE 9th Conference on*, pp. 1756–1761, IEEE, 2014.
- [120] R. Fletcher and C. M. Reeves, “Function minimization by conjugate gradients,” *The computer journal*, vol. 7, no. 2, pp. 149–154, 1964.
- [121] M. R. Hestenes and E. Stiefel, “Methods of conjugate gradients for solving linear systems,” 1952.

-
- [122] D. S. Kershaw, “The incomplete cholesky-conjugate gradient method for the iterative solution of systems of linear equations,” *Journal of Computational Physics*, vol. 26, no. 1, pp. 43–65, 1978.
 - [123] J. H. Wilkinson, J. H. Wilkinson, and J. H. Wilkinson, *The algebraic eigenvalue problem*, vol. 87. Clarendon Press Oxford, 1965.
 - [124] N. J. Higham, “Analysis of the cholesky decomposition of a semi-definite matrix,” 1990.
 - [125] L. Sun, T. Vidal-Calleja, and J. V. Miro, “Bayesian fusion using conditionally independent submaps for high resolution 2.5 d mapping,” in *Robotics and Automation (ICRA), 2015 IEEE International Conference on*, pp. 3394–3400, IEEE, 2015.
 - [126] T. Ohtsuka and T. Komatsu, “Enhancement of electric conductivity of the rust layer by adsorption of water,” *Corrosion science*, vol. 47, no. 10, pp. 2571–2577, 2005.
 - [127] H. E. Knoepfel, *Magnetic fields: a comprehensive theoretical treatise for practical use*. John Wiley & Sons, 2008.